Q. J. R. Meteorol. Soc. (1991), **117**, pp. 125–150 551.515.81(234.3)

The Papal Front of 3 May 1987: A remarkable example of frontogenesis near the Alps

By HANS VOLKERT[1], LUDWIG WEICKMANN[2] and ARNOLD TAFFERNER[3]

[1]*DLR, Institut für Physik der Atmosphäre, Oberpfaffenhofen, F.R.G.*; [2*]*Giselastraße 7, D-8130 Starnberg*; [3]*Meteorologisches Institut der Universität, Munich, F.R.G.*

(Received 25 July 1989; revised 1 October 1990)

SUMMARY

All available, routinely collected surface data are used to document the development of the 'Papal Front', which crossed southern Germany on 3 May 1987 causing casualities and damage. Objective analyses on isentropic surfaces, initialized with the European aerological data, indicate that the development of the violent mesoscale front, which exhibited squall-line characteristics, began when a distinct mid-troposopheric anomaly of potential vorticity reached the north-western rim of the Alpine arc. The forced uplift ahead of the associated shortwave trough combined with ageostrophic motions due to a jet streak at higher levels apparently provided a trigger for deep convection as was observed over the Alpine foreland. Numerical simulations with a dry hydrostatic model indicate the relative importance of the synoptic-scale forcing and the Alpine orography for the generation of the 'Papal Front'. A westerly 'orographic jet' over the foreland below crest height only develops in the simulation with full Alps and is corroborated by the few mountain wind observations that are available.

A comparison with studies of frontal propagation along other mountain ranges reveals that the routine network in the Alpine region and its surroundings is at least of similar density, but so far hardly used for frontal case-studies. It is concluded that a series of 'routine-data case-studies' could help to determine the variability of frontal progression along the Alps and, thus, provide guidance when assessing the significance of single events, particularly those sampled during special observation programmes.

1. INTRODUCTION

In recent years mesoscale meteorology and especially frontal dynamics have received increasing attention worldwide. Research programmes focusing on the interrelation of synoptic-scale and mesoscale circulations during frontal developments have been conducted in Australia (Ryan *et al.* 1985), New Zealand (Steiner *et al.* 1987), United Kingdom and France (Clough 1987), as well as in Germany and neighbouring countries (Hoinka and Volkert 1987). A British–French field experiment over the English Channel and a German–Austrian one in the foreland† north of the Alps were conducted in parallel during the autumn of 1987. Understanding the orographic modification of cold fronts constitutes a central scientific objective within the German Science Foundation project 'Fronts and Orography'.

Theoretically oriented basic studies were started at the same time using simple numerical models and highly idealized flow situations. Egger (1987) investigated the distortion of fronts near orography with a two-layer model and demonstrated that different mountain shapes give a variety of frontal behaviour although the synoptic-scale forcing is not changed dramatically. For archetypal calculations dealing with the effect that Föhn (i.e. cross-mountain flow) has on an approaching cold front, a three-layer model is necessary (Egger 1989). Pre-frontal Föhn was found to be conducive to an acceleration of the front along the mountain barrier. Hartjenstein and Egger (1990) used a multilayer model to investigate the frontogenetic effect that the mere presence of steep orography can have in a stably stratified atmosphere by inhibiting the geostrophic balance along the front. Common features of all the studies are predictions of an 'orographic jet'

* Retired, formerly with Deutscher Wetterdienst, Offenbach, F.R.G.

† This term is used with the meaning of 'land in front' as in the German word *Vorland*.

and the fact that a synoptic-scale forcing driving the mesoscale flow is either completely neglected or only partially parametrized. The term 'orographic jet' stands for a region of increased windspeed along the barrier, which resembles oceanic currents flowing along steep coastal boundaries and gravity currents ducted along a wall in laboratory experiments (see e.g. Griffiths and Hopfinger 1983). It is clearly desirable to check whether the 'Papal Front' would fit in such idealized situations and whether an orographic jet can be detected from the data, as was indeed suggested by Hartjenstein and Egger (1990), based on a preliminary analysis of the event (Heimann and Volkert 1988).

On Sunday, 3 May 1987, four months prior to the beginning of the German–Austrian experiment, a pronounced cold front passed through Munich* somewhat unexpectedly and approximately six hours after a well-forecast (but not very active) first front. This latter front was named 'Papal Front', as a helicopter transfer for Pope John Paul II had to be cancelled because of severe gusts and heavy precipitation. Three people were drowned when yachts on the Bavarian lakes capsized almost immediately after the sudden onset of strong gales. Structural damage was not particularly severe, but there were reports of fallen trees and of farm shelters being blown over. The abruptness and the vigour of the onset of the downpours can also be deduced from numerous newspaper reports that many football matches in southern Bavaria on that Sunday afternoon could not be finished and had to be abandoned.

The present investigation was motivated by the combination of three factors which briefly were: (i) a general effort to study fronts near orography, (ii) the significant gap between simple theories and complex observed phenomena and (iii) the occurrence of a prominent event just prior to a special observing period. It is known from two preliminary studies, based on some surface observations and a few radiosonde ascents (Heimann and Volkert 1988) and with precipitation analyses from rain-gauge data (Volkert 1989), that the Papal Front affected only an area of mesoscale extent (approximately 250 km in a north–south and 600 km in a west–east direction) and that it underwent a distinct development during its 10-hour existence. Isochrones of the surface front positions revealed a growing bulge accelerating eastward south of the river Danube, which at 14 UTC coincided remarkably well with the eastern rim of a massive cloud complex with low cloud-top temperatures ($<-40\,°C$). At the rim the cloud-top temperature changed by more than 20 K over a distance of less than 5 km (see Fig. 6 of Heimann and Volkert 1988). The peak precipitation intensities below that cloud complex amounted to more than $50\,mm\,h^{-1}$, which is commonly considered as a threshold value for intense convective storms (Austin 1987). After all accessible data had been collected it became apparent that more consistent analyses could be undertaken concerning the surface data. Once the mesoscale evolution at the surface is known, the question arises to what extent it was influenced by synoptic-scale forcing and by the Alpine orography. To this end objective analyses of the European rawinsonde data and numerical simulations were carried out using a three-dimensional adiabatic (dry) hydrostatic model. In short, the aims of this study are:

(i) the detailed documentation of the synoptic-scale environment and mesoscale development, taking into account all available routinely collected data;

(ii) the assessment of the relative importance of synoptic-scale forcing and Alpine orography upon the mesoscale development over the foreland north of the mountains; and

* The semantic problem arising from geographic names with English and German versions is dealt with in the following way. In the text the English version is used (e.g. Munich, Constance), whereas the German form of the names appear in the tables and figure captions (e.g. München, Konstanz).

(iii) a clarification of whether a low-level jet along the mountains occurred and if so whether it could be attributed to the Alpine influence.

Pursuit of these aims serves several purposes. For example, (a) better observational evidence is available to check results and the validity of theoretical studies; (b) the quality and limitations of routinely collected data are considered, e.g. for comparisons with analyses of data originating from special campaigns (see e.g. Hoinka *et al.* 1990; Kurz 1990); and (c) the interrelation between between the synoptic-scale flow in the upper troposphere and orographically influenced mesoscale structures at lower levels is demonstrated.

The organization of the paper is as follows. In section 2, we look briefly at related observational studies. Section 3 is devoted to analyses of the surface data, and section 4 deals with the upper-air synoptic-scale environment. Concluding remarks, which also mention some inevitable shortcomings of this case-study, make up section 5.

2. Related studies

Fronts are an important factor in the weather and climate of the Alpine foreland, which they cross on about 75 days each year (ten-year average) causing approximately 50 per cent of the annual precipitation (Hoinka 1985). Thus, one might expect some detailed case-studies of prominent events at least, especially as 'a fairly dense meteorological network existed already' (GARP 1986, p. ix). However, few studies have been published during the last 40 years.

Staude (1970) investigated a severe hailstorm which occurred on 6 July 1968 approximately 50 km west of Munich. After concentrating on local observations (e.g. time-series, area of damage) he presented mesoscale surface charts which exhibit surprising similarities with our analyses although only 17 stations were used (his Figs. 8, 9; our Fig. 2). The hail-producing thunderstorm developed at a cold front which crossed southern Germany ahead of a strengthening mesoscale high. An Alpine influence was not mentioned.

Steinacker (1987), focused on fronts and orography, where orography in his cases meant the entire Alps. Three very instructive examples indicate how the Alpine massif can block the progression of a surface cold front towards the south-east; a fourth one shows to what extent the upper tropospheric front is less influenced than the surface front. For these regional weather charts, data came from synoptic stations (3-hourly) and rawinsondes (6-hourly; ALPEX period).

Case-studies of frontal propagation along other mountain ranges are available for the Australian Alps (Colquhoun *et al.* 1985), the Pyrenees (Hoinka and Heimann 1988), both sides of the Rocky Mountains (Mass and Albright 1987; Shapiro *et al.* 1985), and the Appalachian Mountains ('back-door' fronts, Carr 1951; Bosart *et al.* 1973, give a detailed climatology of 'back-door' frontal passages).

Colquhoun *et al.* (1985) provided the synoptic background for two 'southerly buster' cases, a particularly intense type of orographically and thermally influenced cold front which occurs quite frequently in spring and summer along the southern part of the east coast of Australia. These authors presented isochrones of the frontal positions which showed the propagation along the coast and the retardation over the mountains. Hoinka and Heimann (1988) detected an eastward movement of a distinct tongue of low-level cloud at the northern edge of the Pyrenees using satellite imagery, and related it to the progression of a surface cold front which was analysed from 3-hourly reports of a synoptic station network. Mass and Albright (1987) discussed in considerable detail two cases in which surges of cool air, marked by stratus and fog, travelled northwards along the

TABLE 1. NUMBER OF SURFACE STATIONS (n), AREA OF INTEREST (F), AVERAGE DISTANCE BETWEEN STATIONS ($d = (F/n)^{1/2}$), AND PERIOD (T), DURING WHICH THE FRONT TRAVERSES F, FOR SEVERAL STUDIES OF FRONTS MOVING ALONG OROGRAPHY

Authors	Mountain range	n	F (km^2)	d (km)	T (h)
Colquhoun *et al.* 1985 (Fig. 8)	Australian Alps (eastern edge)	22	60 000	50	11
Hoinka and Heimann 1988 (Fig. 2)	Pyrenees (northern edge)	23	120 000	70	18
Mass and Albright 1987 (Fig. 10(a))	Pacific Coastal Mountains (western edge)	49	360 000	85	—[1]
Shapiro *et al.* 1985 (Fig. 4)	Rocky Mountains (eastern edge)	22	27 000	35	3
Staude 1970 (Figs. 8, 9)	European Alps (northern edge)	17	120 000	85	—[2]
Steinacker 1987 (Fig. 1)	European Alps (entire)	300[3]	700 000	50	48
This study (Fig. 3)	European Alps (northern edge)	85[4]	135 000	40	8

[1] No isochrones, but moving mesoscale charts over a period of 36 h
[2] No isochromes, but two mesoscale charts separated by 3 h
[3] Varies with time of observation between 127 and 369
[4] Varies with time of observation between 57 and 90

western side of the Pacific coastal mountains. Shapiro *et al.* (1985) documented a very sharp, non-precipitating front which moved southwards along the eastern edge of the Rockies and thereby passed a dense meso-network and an instrumented 300 m meteorological tower.

Besides the obvious influence that the orography had on the frontal propagation in the above-mentioned cases, all these fronts were only a few hundreds of kilometres long; none of them was properly resolved on regular weather charts. In Table 1 an attempt is made to quantify the area of interest and the number of available surface stations from the cases studied. The areas differ by a factor of 40, from eastern Colorado to the entire Alpine region, and the average distance between stations varies between 35 and 85 km. Although these figures are only estimates, they illustrate the range of scales which are commonly ascribed to 'mesoscale'*. We note that isochrone analyses certainly depend on the network density and that careful timing becomes increasingly important as the distance between stations is reduced (e.g. in a 40 km network a disturbance travelling at 15 m s^{-1} needs less than one hour to pass from one station to the next). Furthermore, it is evident that the Alpine region offers a quite dense routine network.

3. MESOSCALE ANALYSES OF SURFACE DATA

In this section, we analyse the structure and the development of the Papal Front over southern Germany and the adjacent countries as reflected in surface data. The area of special interest, to which most of the observations are restricted, is bounded by longitudes 7 and 14°E and latitudes 47 and 49.5°N, whereas our original analyses were carried out beyond these bounds.

Figure 1 gives some impression of the complex topography within the area of special interest. In its western part, the low region of the Rhine valley is surrounded by the

* We apply the terms 'synoptic-scale' to horizontal extents of between 250 and 2500 km and 'mesoscale' to lengths between 25 and 250 km; they are synonymous with the occasionally used terms 'meso-α' and 'meso-β' scales, respectively.

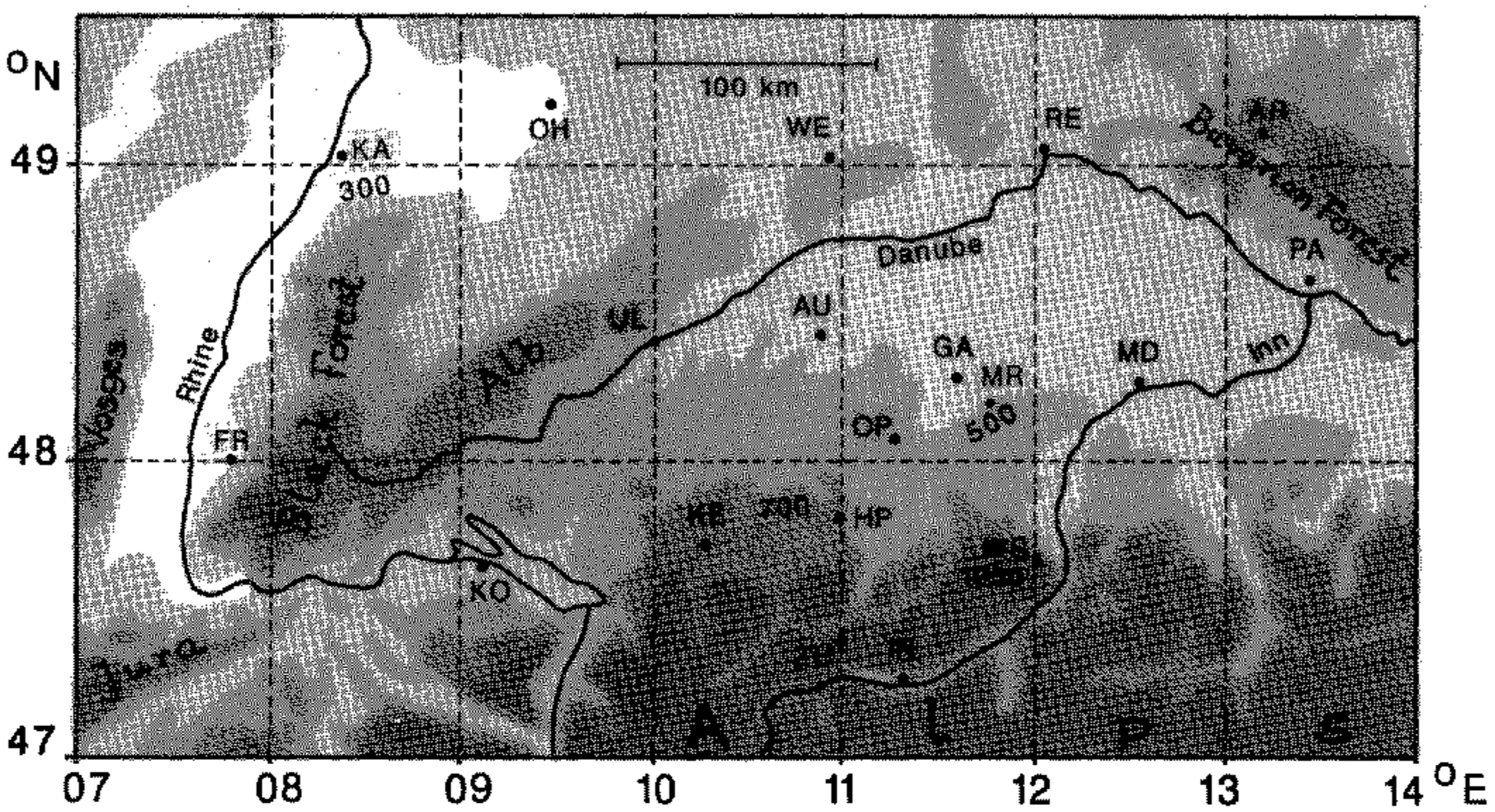

Figure 1. Area of special interest containing the northern edge of the Alps and the pre-Alpine region. Grey scale according to elevation (threshold values: 300, 500, 700, 1000 m). Two-letter codes designate stations mentioned in the text: AR–Gr. Arber; AU–Augsburg; GA–Garching; FR–Freiburg; HP–Hohenpeißenberg; KA–Karlsruhe; KE–Kempten; KO–Konstanz; IN–Innsbruck; MD–Mühldorf; MR–München-Riem; OH–Öhringen; OP–Oberpfaffenhofen; PA–Passau; RE–Regensburg; UL–Ulm; WE–Weißenburg; WS–Wendelstein; ZU–Zugspitze.

French Vosges, the Swiss Jura and the German Black Forest, which extends as the Swabian Alb towards the north-east. The Alpine baseline may be defined as the envelope of the northernmost positions of the 100 m contour. The north-Alpine foreland gradually descends towards the river Danube, which is flanked on its left bank by a chain of hills including the Bavarian forest downstream from Regensburg.

The synoptic-scale surface analysis for 12 UTC, 3 May 1987 indicates an elongated frontal zone with several waves extending from Spain over northern Italy towards Poland, Finland and beyond (cf. the European Meteorological Bulletin, DWD, Offenbach). Our region of special interest is represented by only two stations, although some more may have been used for the original analysis. The regional chart for central Europe in the Berliner Wetterkarte (Institute of Meteorology, Free University, Berlin) covers 22 stations in that area. It depicts the same frontal zone but in a less advanced position. In its rear, over the Black Forest/Swabian Alb and northern Switzerland, a zone of an enhanced west-to-east pressure gradient is evident with reports of rain, snow and thunderstorms. The Papal Front, not identified in these charts, is the evolving line of discontinuity at its leading edge, which we are to diagnose in more detail. But before doing so, we note that already at 00 UTC a double structure could be seen in the field of equivalent potential temperature at the 850 hPa pressure level where maritime polar air was sandwiched in between a warm subtropic airmass over the Alps and Italy and a cold maritime arctic airmass spreading towards northern France (cf. Berliner Wetterkarte and Heimann and Volkert 1988, Fig. 1).

Within the region of special interest, the present investigation uses all weather reports available from regular and auxiliary stations to manually construct hourly surface analyses between 08 and 18 UTC, as well as at 21 UTC. Three examples are given in Fig. 2 for the times 09, 12, 15 UTC, respectively. We recognize the surface pressure trough of

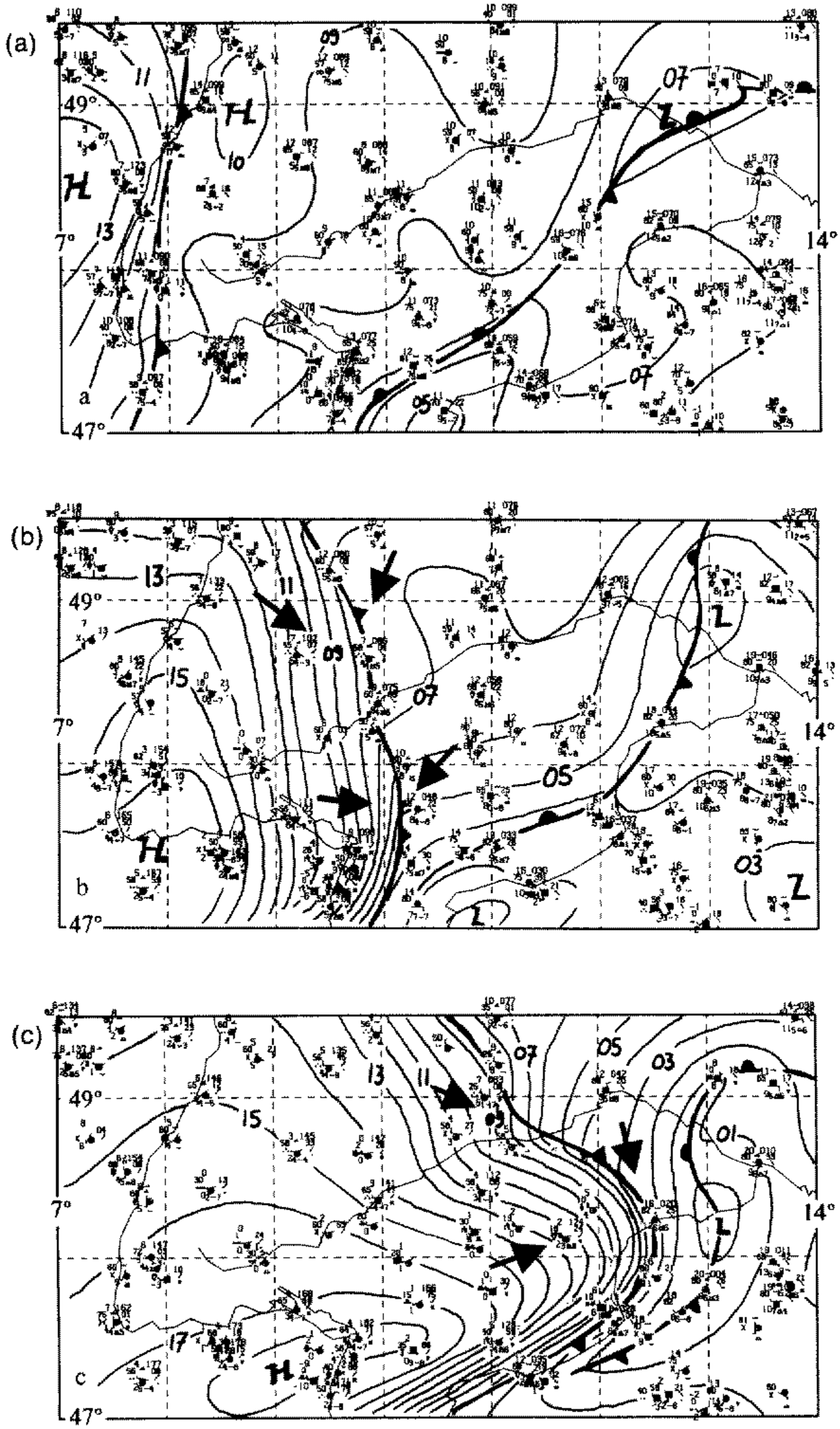

Figure 2. Mesoscale surface charts for 3 May 1987: (a) 09 UTC, (b) 12 UTC, and (c) 15 UTC. 1000 hPa has to be added to the isoline labels; pressure increment: 1 hPa (behind the Papal Front in (c): 2 hPa). Thick arrows highlight observed wind directions.

the synoptic-scale analyses with minor waves over the eastern part of the domain and its slow eastward progression. At the leading edge of the intensifying meso-high, the Papal Front is analysed as a cold front. It is marked by a pronounced confluence, a zone of distinct temperature gradient and of active weather (rain, snow, showers, thunderstorms). The isobars are nearly parallel to the Papal Front at its rear where the winds have a marked cross-isobaric (i.e. ageostrophic) component. Within the evolving bulge, just off the Alpine baseline, the surface flow is in some places at right angles to the isobars. At 15 UTC, the cold front was just about to enter the pressure trough and thus had almost caught up with the frontal zone from the synoptic-scale analyses. As the reduction of pressure to sea level takes into account the temperature observed at the particular station, the pressure gradient across the Papal Front may have been overestimated by up to 3 hPa because of the cross-frontal temperature contrast (up to 20 K) and a mean elevation of 500 m. The mesoscale pressure difference is up to six times as large and the pressure pattern is not influenced by the pressure reduction.

The hourly positions of the Papal Front are displayed in Fig. 3. Most noteworthy is the bulge in the vicinity of the forty-eighth parallel, where the average hourly speed of the front doubled within four hours, and the retardation of the front over the Alps. The passage time of the Papal Front in Linz (Austria; 48°14′N, 14°11′E) and St. Pölten (Austria; 48°12′N, 15°37′E; 55 km to the west of Vienna) and weather reports from Austria and Czechoslovakia, all outside the area of special interest, reveal that the bulge progressed eastwards with about the same speed and shape and with only minor widening in the meridional direction. Figure 3 is more consistent than the result of a similar analysis given in Heimann and Volkert (1988, Fig. 5) as local passage times of the front determined from wind recordings (see Fig. 5) have been taken into account. Although the isochrones in Fig. 3 are derived manually, we believe that they represent the most consistent result that can be expected from the kind of data available and their spatial density. Shape and position of the 14 UTC position of the front coincide well with the leading edge of the above-mentioned cloud complex, as seen by the NOAA-9 satellite at 1415 UTC (see Heimann and Volkert 1988, Fig. 6).

Having identified the progression of the Papal Front we now concentrate on its intensity. It is obvious from Fig. 2 that the pressure gradient across the front, and the

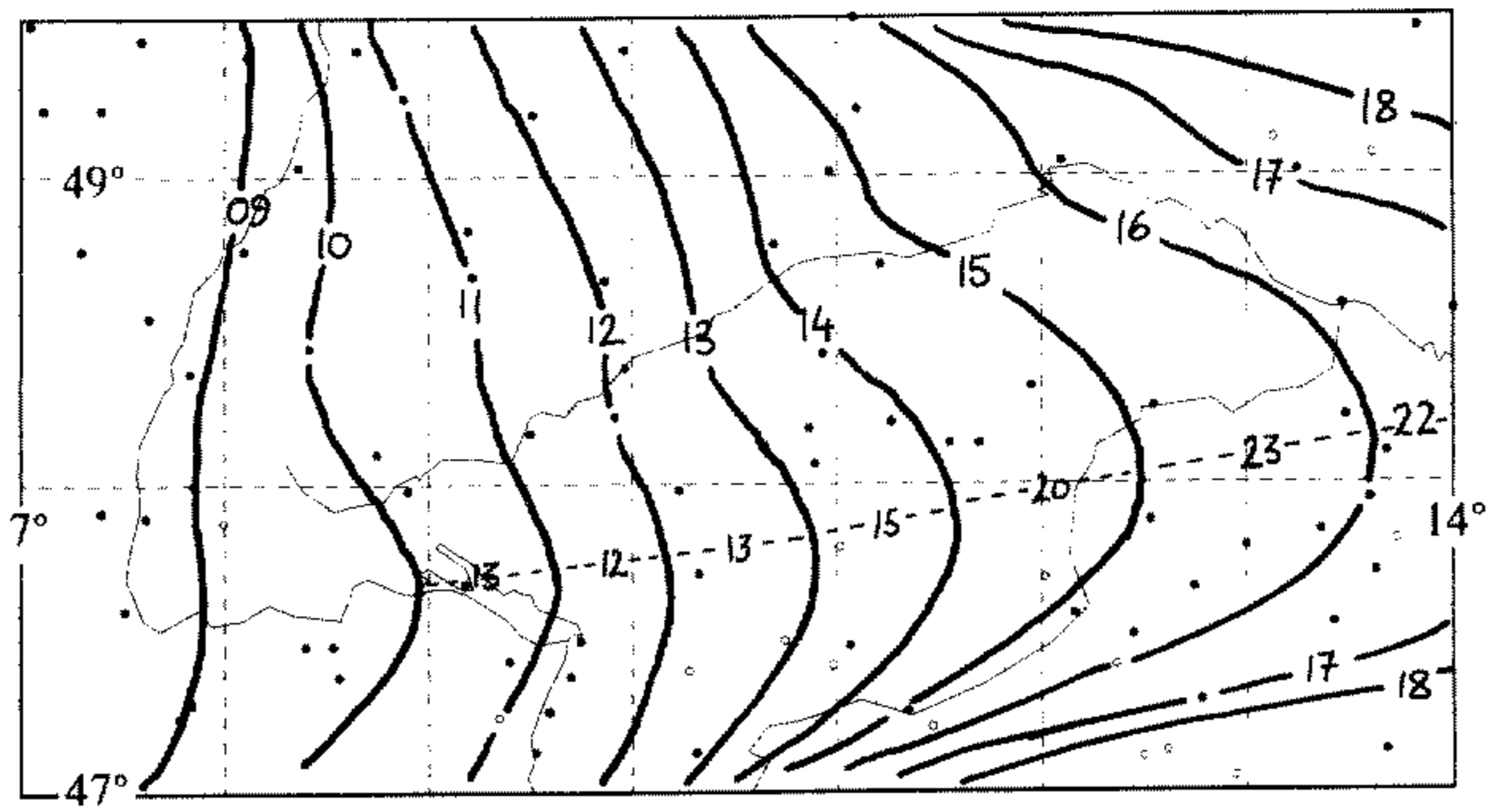

Figure 3. Hourly isochrones of the surface front positions from 09 to 18 UTC. Dots indicate reporting stations at 12 UTC; open circles denote the subset of mountain stations above 800 m. The average hourly speed (in $m\,s^{-1}$) of the bulge is given along the dashed line. The speed between 16 and 17 UTC is extracted from an extended chart.

temperature difference both increased with time. This intensification of the Papal Front becomes even more evident from a comparison of time-series obtained at the meteorological towers in Karlsruhe (passage of the front at 0940 UTC; sampling interval: 10 min; Fig. 4(a)) and in Garching, 15 km north of Munich (passage of the front at 1420 UTC, sampling interval: 2 min, Fig. 4(b)). In Karlsruhe, all meteorological variables exhibited comparatively smooth transitions. A wind shift from north to west was accompanied by an increase in speed and a distinct change in the decrease of temperature. Relatively steady rainfall set in half an hour later (approximately 3.5 mm h^{-1} over one hour). In Garching, four hours later and some 200 km further east, sudden discontinuities are apparent. The windspeed had tripled, the pressure jumped by 2 hPa before increasing another 5 hPa. Within six minutes the temperature dropped by 6.2 K, and 3.1 mm of rain reached the ground. Later on, the precipitation turned into snow. The equivalent potential temperature, often used as an airmass marker, dropped by 12 K within six minutes and further decreased by 9 K during the following 1.5 hours. The passage of the preceding synoptic-scale front is clearly marked in the windspeed and temperatures (equivalent potential, dry and dew-point) at 0825 UTC, and shows no precipitation. This time is consistent with the mesoscale analysis in Fig. 2(a). In the records from Karlsruhe this earlier front is not displayed, as it passed there on the previous day.

We note that the traces from Garching (and, less pronounced, those from Karlsruhe; Fig. 4) offer some insight into the Papal Front's internal structure. Wind and temperature

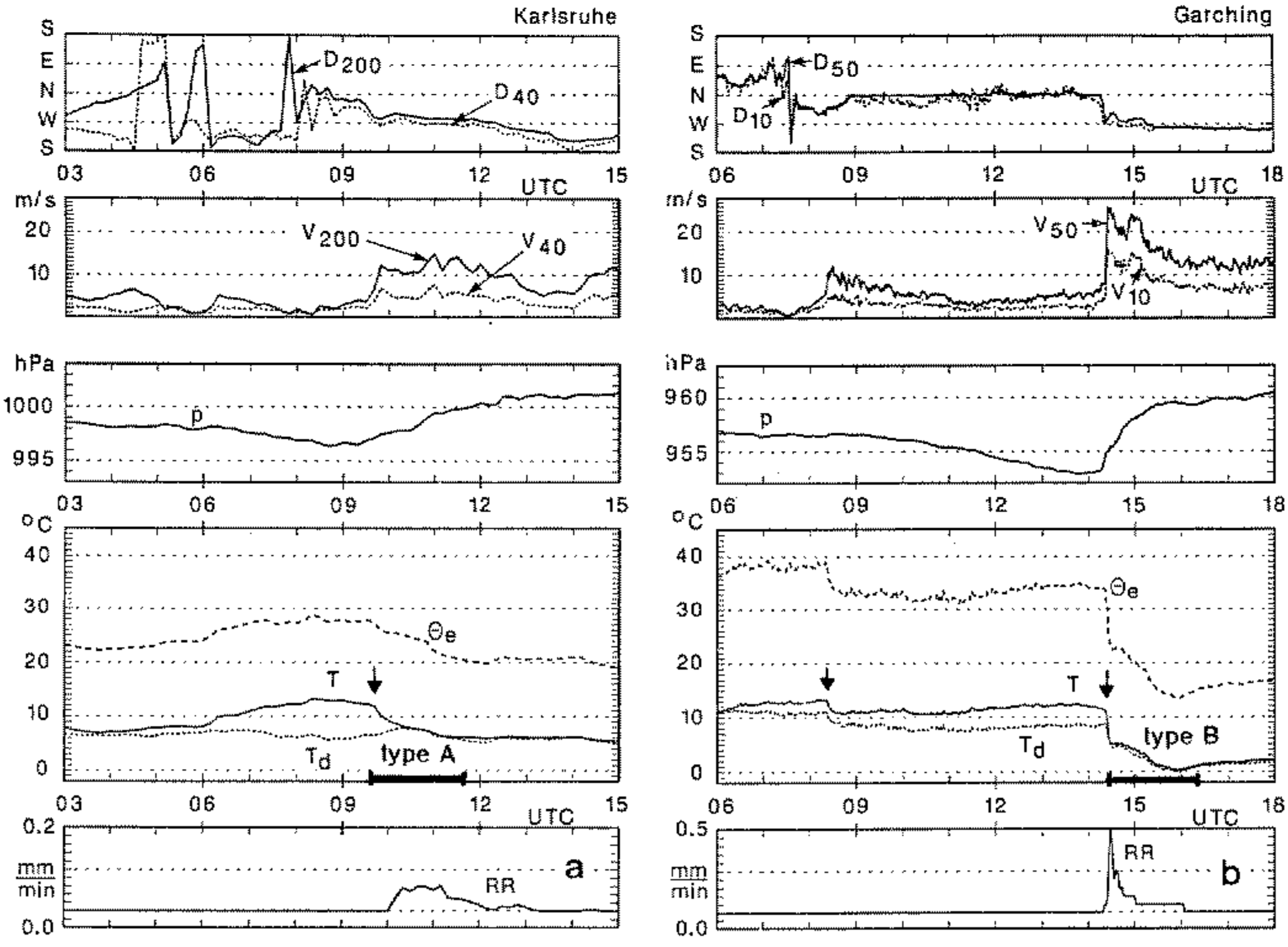

Figure 4. Time series of digital observations from Karlsruhe (sampling interval: 10 min) and Garching (sampling interval: 2 min) recorded on 3 May 1987. The symbols stand for (from top to bottom): wind direction *xx* m above ground (D_{xx}); wind speed *xx* m above ground (v_{xx}); pressure (p); equivalent potential (θ_e), dry (T), and dew-point temperatures (T_d) at 2 m above the ground; precipitation rate (RR). Frontal passages are marked by arrows in the temperature trace; the '2-hour bar' following the drop in temperatures serves as reference for Table 2 (see text).

data exhibit a double structure. The first gust and the sudden temperature drop (at 1420 UTC) are clear signatures of a squall (or gust front) at the leading edge of a cold air outflow passing a fixed location (see e.g. Mahoney 1988, Fig. 5). A second wind maximum occurred half an hour later concurrently with the beginning of a more gradual decrease of temperature which followed the sudden drop. Evaporative cooling and especially melting of snow within the body of the post-frontal airmass (as opposed to the leading squall) had supposedly played a significant role in achieving the overall reduction in temperature (more than 20 K in 24 h, including the preceding synoptic-scale front) and for generating such an energetic and fast-moving system.

As indicated in Fig. 4, for the temperature evolution after the passage of the Papal Front we qualitatively distinguish between the early type A signature (gradual decrease of temperature following a distinct kink in the trace—as in Karlsruhe) and the developed type B structure (sudden drop followed by a more gradual further temperature reduction). Although the Papal Front progressed with acceleration, the difference between the temperature records in Karlsruhe and Garching cannot be explained by increased frontal speed alone. Moreover, the records show that any contribution of daytime heating ahead of the Papal Front was very small, if it existed at all. Obviously considerable frontogenesis had taken place during the interval of well over 200 km in distance and more than 4 hours in time. Of course, the front did not travel straight from Karlsruhe to Garching (see Fig. 1); thermograms can be used to gain a better spatial resolution, although the temporal resolution is much poorer compared to the electronically sampled data.

Thermograms are available from 13 stations (weekly records). In forming an estimate of the temperature change with time for the Papal Front we found a two-hour interval appropriate for two reasons: (a) it contained virtually all of the temperature decrease in Karlsruhe and in Garching, and (b) it can be easily read from the recordings. The findings are collected in Table 2. The drops in temperature consistently increased in size from west to east and were least pronounced at the northern edge of the area of special interest. Both electronically and conventionally measured values agree well with each

TABLE 2. MAXIMUM WIND SPEED, v_{max}, MOSTLY FROM ANEMOGRAMS; PASSAGE TIME OF PAPAL FRONT, t_0, TO THE NEAREST 5 MIN (SEE FIGS. 4, 5); AMOUNT, $\Delta T/\Delta t$, AND TYPE OF TEMPERATURE CHANGE (SEE TEXT) AFTER PASSAGE AT THREE GROUPS OF STATIONS (SEE FIG. 1)

Group	Station	Code	v_{max} ($m\,s^{-1}$)	t_0 (UTC)	$\Delta T/\Delta t$ (K/2 h)	Type
West	Karlsruhe	KA	8[1]	0940	−6	A
	Öhringen	OH	18	1150	−6	AB
	Freiburg	FR	13	0900	−6	A
	Konstanz	KO	21	1015	−5	AB
Middle	Weißenburg	WE	19	1400	−6	A
	Ulm	UL	14	1220	−6	A
	Augsburg	AU	21	1320	−8	B
	Garching	GA	26[2]	1420	−11	B
	München-Riem	MR	24	1415	−12	B
	Kempten	KE	19	1220	−11	B
	Innsbruck	IN	20	1440	−11	B
East	Regensburg	RE	26	1620	−7	A
	Mühldorf	MD	25	1510	−12	B
	Passau	PA	25	1610	−15	B
	Linz (Austria)	—	27	1635	−13	B
	St. Pölten (Austria)	—	26	~1830	−12	B

[1] 10 min value at 40 m above ground
[2] 2 min value at 50 m above ground

other. Type B structures with temperature drops of 10 K or more were restricted to the region south of the river Danube and east of the tenth meridian, culminating in Passau. In the records from Öhringen and Constance, situated in the formation area of the Papal Front, a sudden drop of about 2 K appeared in the middle of the gradual decrease. It is classified as type AB and can perhaps be interpreted as the result of an outflow from a local storm during the time before the Papal Front became an organized entity of mesoscale extent.

Additionally, the maximum gusts at or after the front and the times of frontal passage are given in Table 2. The latter were taken from anemograms (daily records), as the thermograms do not give very precise timing. Nine examples of windspeed charts (gusts) are given in Fig. 5. The passage time (indicated by an arrow) is determined by the onset of the wind squall and the sudden change in wind direction (not displayed). The anemograms show the variability of the Papal Front's wind squall within the area of special interest (see Fig. 1). General characteristics are the increase in strength from west to east and the most pronounced rate of change in windspeed in the plain just outside the Alpine baseline (as in Kempten). These effects, incidentally, continue at least as far as St. Pölten (Austria) where a significant type B temperature drop (12 K in 2 h) was recorded at about 1830 UTC with a maximum gust of 26 m s^{-1}. For the total distance between Freiburg and St. Pölten (about 575 km) an average speed of 60 km h^{-1} (17 m s^{-1}) is obtained, with a maximum of about 80 km h^{-1} (22 m s^{-1}) in the region south of Passau.

As an additional source of routinely collected data a network of recording rain gauges (mainly Hellman type; daily chart) is used to identify onset times of significant precipitation and to quantify the precipitation intensities in the wake of the Papal Front. Details of the quality of the data, the digitization of the 135 stripcharts obtained from the area of special interest (extended to 50°N; see Fig. 6) and a collection of time–intensity histograms can be found in Volkert (1989). For the current investigation, the recordings were subjected to further scrutiny on the basis of areal charts (not displayed) which permitted the correction of time errors, i.e. confusions between UTC, Central European Time (UTC + 1 h) and Daylight Saving Time (UTC + 2 h), as well as the elimination of recordings with obvious clockwork or other technical failures. Eventually, 125 recordings were taken into account.

As displayed in Fig. 6, the precipitation-onset isochrones north of the river Danube were well ahead of the Papal Front and not connected with any surface front. The precipitation intensities were below the 10 mm h^{-1} level. Precipitation connected with the Papal Front shows up as a secondary kink some time after the onset time in the southern part of this area. South of the river Danube the onset isochrones correspond very well with those of the surface-front position (see Fig. 3), especially if one bears in mind the lag of about 20 min between the nominal times of synoptic observation and the actual readings or registrations. Precipitation intensities in the wake of the Papal Front were one order of magnitude higher than in the north, reaching peaks of more than 100 mm h^{-1} for durations of a few minutes.

Although the overlap between pre-frontal rain and the 'Papal Front downpours' contains subjective judgement at some stations, the distinction of two eastward-moving precipitation patterns appears to be significant. It is surmised that synoptic-scale lifting processes as observed ahead of shortwave troughs initiated the rainfall north of the river Danube, while south of it considerably stronger vertical motions caused the eastward accelerating downpour.

The evolution of the heavy rainfall over southern Bavaria is displayed in Fig. 7 by a time–distance diagram from Lake Constance (Langenargen—LA; 0 km) to the con-

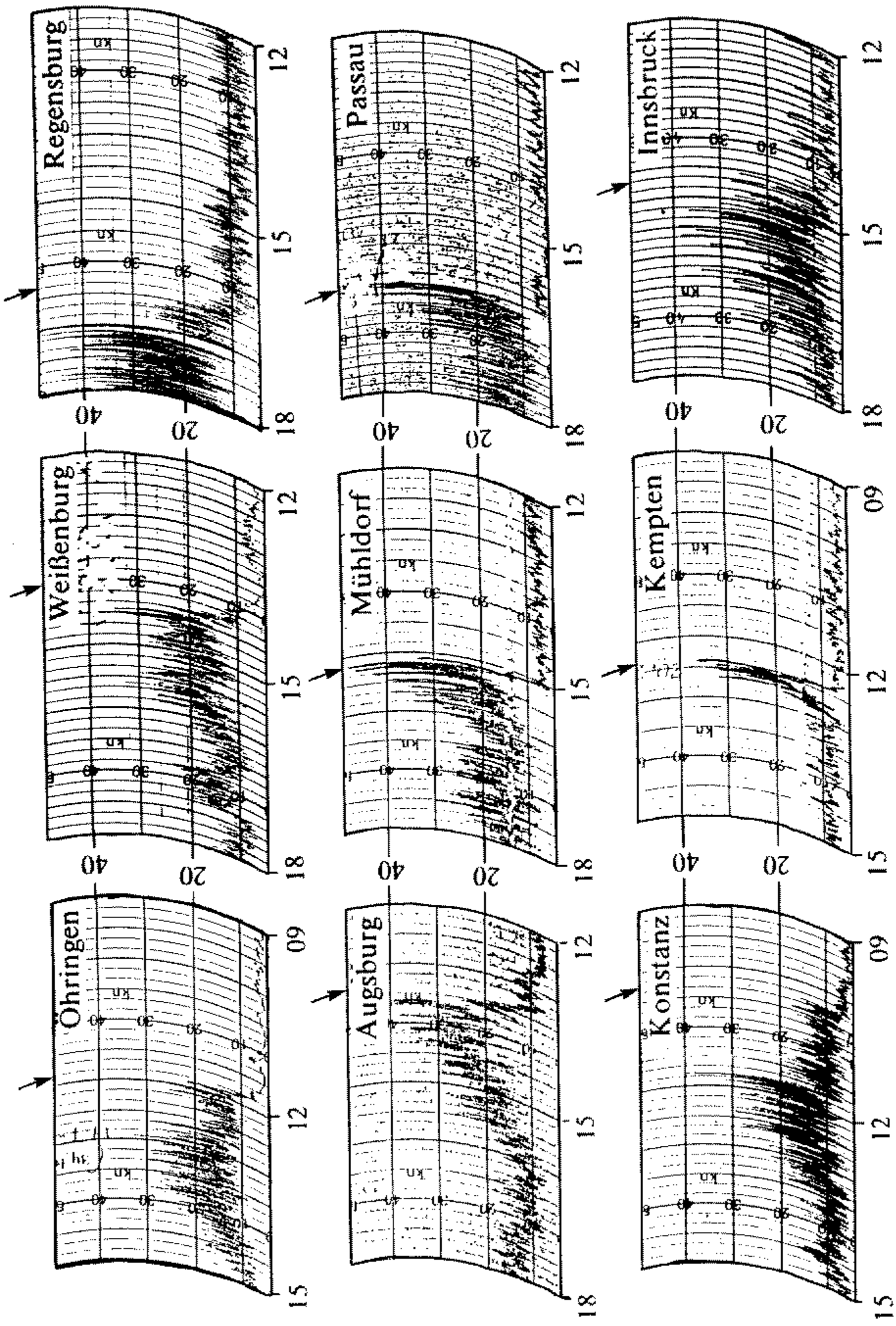

Figure 5. Anemograms of maximum wind speed (gusts; in knots) for nine stations from north (top) to south and from west (left) to east (see Fig. 1 and Table 2); times in UTC. The arrows above the frames denote the passage time of the Papal Front consistently derived from the wind direction traces (not displayed).

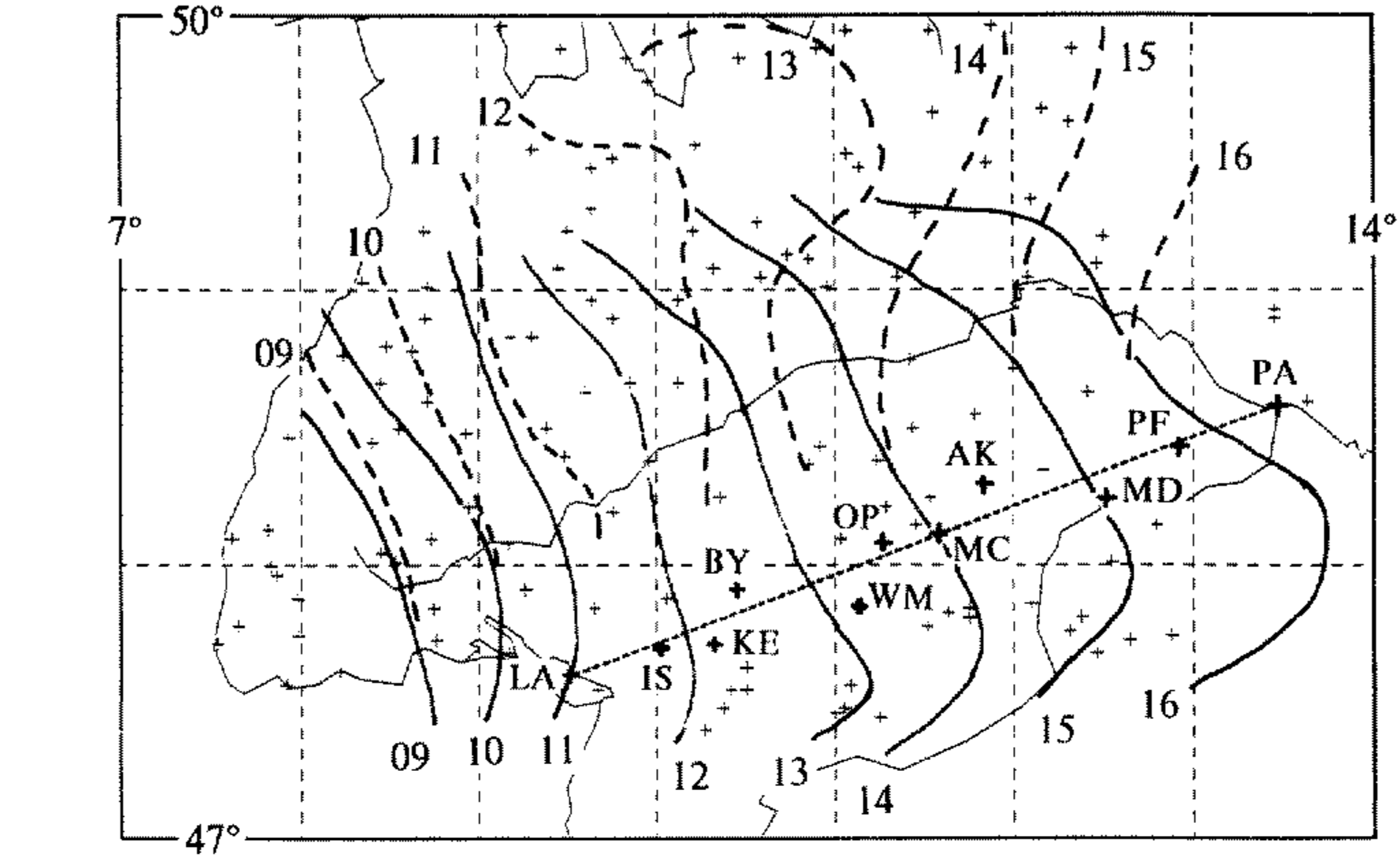

Figure 6. Onset times (UTC) of two kinds of precipitation over southern Germany on 3 May 1987: pre-frontal rain (dashed lines; mainly in the north) and precipitation connected with the Papal Front (full lines; mainly in the south). Crosses denote station network; those in bold and annotated along the dashed line define the cross-section displayed in Fig. 7. Station codes (from west to east): LA–Langenargen; IS–Isny; KE–Kempten; BY–Bayersried; WM–Weilheim; OP–Oberpfaffenhofen; MC–München City; AK–Aufkirchen; MD–Mühldorf; PF–Pfarrkirchen; PA–Passau.

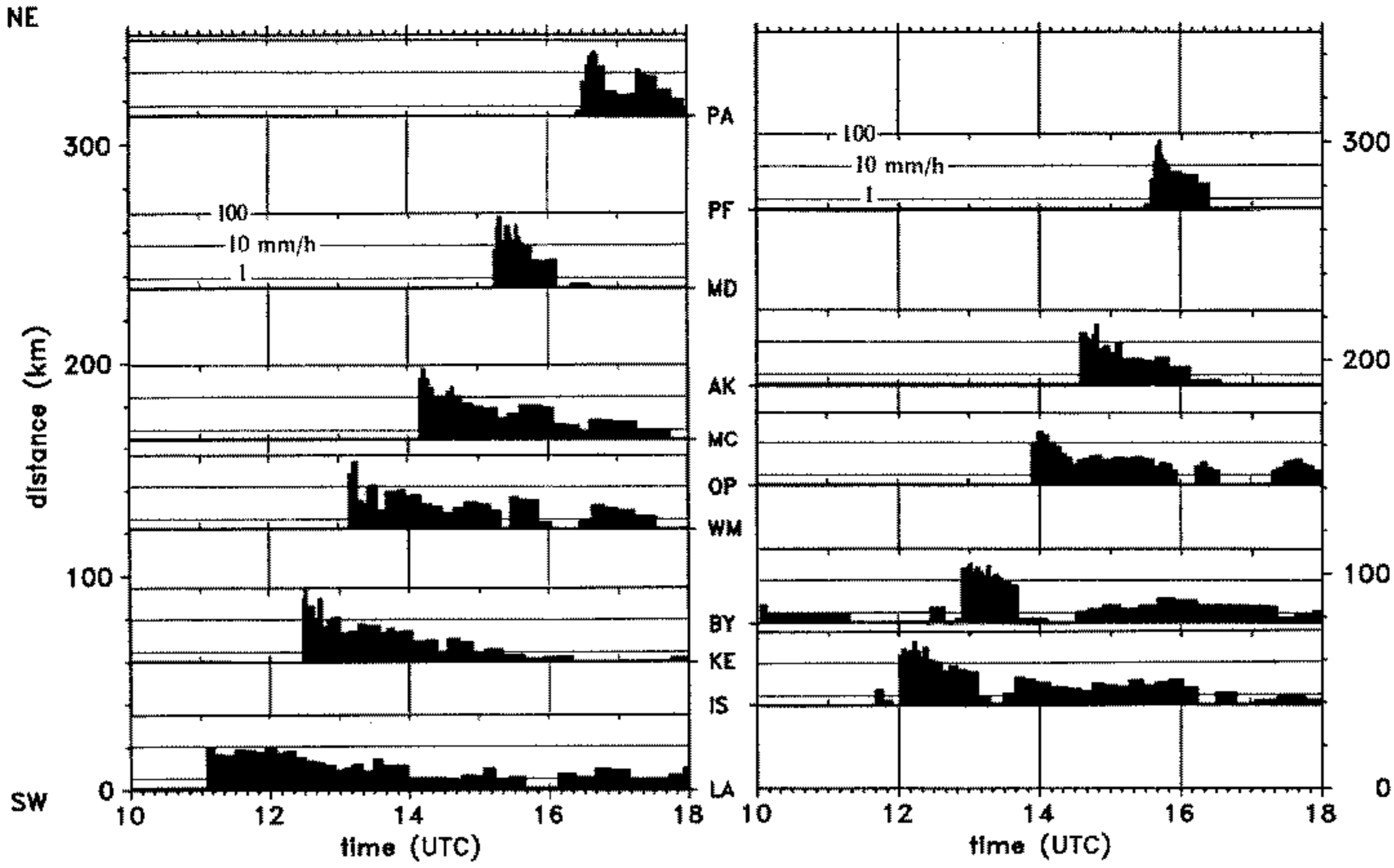

Figure 7. Time–distance diagrams of precipitation intensities along the line Langenargen (LA)–Passau (PA) defined in Fig. 6. To gain vertical space for the histograms the geographical sequence alternates between the left and right diagram. The scale in each histogram is logarithmic from 0.5 to 100 mm h^{-1} with 1 and 10 mm h^{-1} as intermediate levels. Station codes are as given for Fig. 6.

fluence of the rivers Danube and Inn (Passau—PA; 315 km). The main development took place over the first 60 km with an increase in onset intensity from 9 mm h^{-1} (Langenargen) through 45 mm h^{-1} (Isny) to 280 mm h^{-1} (Kempten; the peak rate observed was 7 mm in 1.5 min). From then onwards, the downpour moved quite uniformly and roughly parallel to the Alpine baseline with peak intensities, varying between 20 and 70 mm h^{-1}, always observed shortly after the onset of precipitation. These intensities fall into the class of intensive convective storms as defined by Austin (1987, p. 1061; peak intensities over 50 mm h^{-1}). Instead of multiple precipitation line-elements separated by gaps, which lead to quite variable rain-gauge readings at different stations (see James and Browning 1979), the Papal Front was followed by a single downpour of about 2 h duration with an areal extent of at least 300 km × 100 km.

It is interesting to note that the 6-hourly precipitation totals (12 to 18 UTC) amounted to about 15 to 20 mm over the foreland with a slight but systematic decrease towards the east and much reduced values inside Alpine valleys. So, when the Papal Front accelerated and developed a stronger temperature contrast at the surface, it did not enhance its precipitation intensity or efficiency. This may be judged as indirect evidence that the system was triggered over the western part of our area of interest (or even further to the south-west), then organized itself as a complex of deep precipitating convection of a size sufficiently large to move along the Alpine boundary under the influence of its own dynamics, even when thermodynamic processes (roughly estimated from the precipitation amount reaching the ground) became weaker.

Reflectivity measurements by radar serve as a standard means of determining the extent and progression of precipitation complexes. Because of a technical failure on the previous day, the weather radar which is situated on the Hohenpeißenberg (see Fig. 1) and is equipped with a data storage device, was out of order. Therefore, the only available images are those obtained from the Swiss radar, which is located on the Albis hilltop (923 m; for technical details see Joss and Waldvogel 1990, particularly p. 602). They document three projections (ground view, W–E and N–S cross-sections) of maximum reflectivity with a horizontal pixel size of 2 × 2 km^2 and a vertical resolution of 1 km using seven reflectivity intervals and a time discretization of 10 min.

The temporal evolution of the distinct precipitation complex, which marks the initial phase of the analysed downpour, is shown in Fig. 8. During the morning hours, Switzerland was covered by patchy reflectivity patterns of below 33 dBZ intensities and very few small and non-persisting cells of higher intensity (probably local showers). At 1125 UTC two such cells appeared above the upper Rhine valley close to the north-eastern edge of the area of low reflectivity. Ten minutes later, both cells had merged to become the size given in Fig. 8 (core 1). Over the following 80 min this reflectivity maximum increased in intensity (highest value between 48 and 55 dBZ at 1225 UTC between 3 and 4 km a.m.s.l. just south of Kempten) and in vertical extent (33 dBZ threshold at 6 km a.m.s.l. over a meridional distance of about 60 km at 1315 UTC). It progressed rather uniformly at a speed of about 50 km h^{-1} (14 m s^{-1}). This value is close to but slightly higher than the average speed of the surface front during the same period (see Fig. 3). Allowing a systematic timing difference of 15 min between radar, rain gauge and synoptic data, or location errors of the reflectivity cores of about 15 km (pictures of the radar screen on 16 mm film are the only available data source) and taking into account the different reference heights of surface and radar data we conclude that all three data sources, as displayed in Figs. 3, 7 and 8, give consistent evidence.

In summary, we note that the precipitation complex, which crossed southern Bavaria during the afternoon of 3 May 1987, formed over the upper Rhine valley at or closely behind an analysed surface front. It intensified during the following hour while propa-

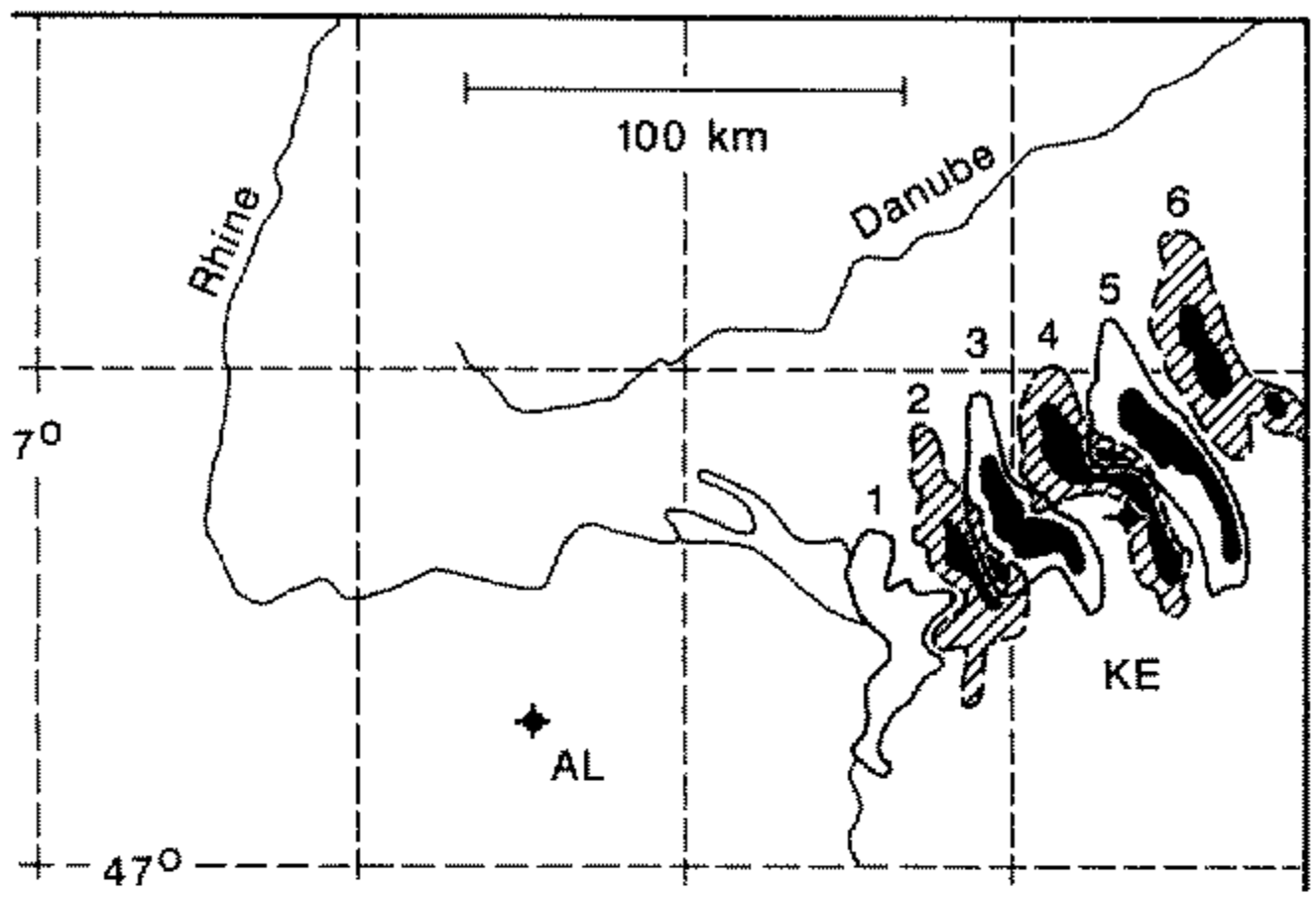

Figure 8. North-east corner of the area seen by the Swiss radar located on the Albis (AL). Displayed is the progression of echo cores ($\Delta t = 20$ min; 1: 1135 UTC; . . .; 6: 1315 UTC). The outer threshold (alternating full/dashed lines around white/hatched areas) equals 33 dBZ, the inner one (boundary of black areas) 40 dBZ. The dotted cross (KE) at the edge of core 4 shows the location of Kempten (see (Fig. 1); the dashed lines indicate the latitude–longitude grid.

gating along the rim of the Alps at a speed similar to that of the surface front. Maximum radar echoes and the highest precipitation rate were observed in the vicinity of Kempten. The size of the reflectivity core (>33 dBZ) remained remarkably constant over the 80 min period before it left the radar range, much unlike the initial phase of a well-documented mesoscale convective complex in the same area (see Höller and Reinhardt 1986, Fig. 3 (e–h)). This could be explained by a synoptic-scale dynamical ascent taking precedence over more localized thermo-dynamical forcing from the ground.

Numerical studies using idealized flow situations along orography predict a low-level jet behind a front near the obstacle (e.g. Hartjenstein and Egger 1990), as has been recorded in the case of other mountain ranges (see e.g. Parish 1982, for the Sierra Nevada in the south-western United States). The accelerating bulge in the surface-front isochrones (see Fig. 3) gives some indication that indeed an orographic jet may have been present in the wake of the Papal Front. As no post-frontal wind sounding is available, we use the surface winds from stations of different elevations to check that presumption. Table 3 shows hourly synoptic wind reports (10 min averages) for five stations of heights between 500 m and 3000 m a.m.s.l. up to three hours after the Papal Front had passed. The highest values are found at the 1400 m level, a height well above the Alpine foreland but below the crest height of the Alps. So, the existence on 3 May 1987 of an orographic jet is corroborated by the few observations available. Whether its meridional extension as far as the Bavarian Forest (Gr. Arber is situated approximately 150 km north of the Alpine baseline) is exceptional, remains an open question.

TABLE 3. HOURLY SYNOPTIC WINDSPEED REPORTS (KNOTS; 10-MIN AVERAGES; BRACKETED VALUE INTERPOLATED FROM NEIGHBOURING HOURS) ON 3 MAY 1987 AFTER THE PASSAGE OF THE PAPAL FRONT AT FIVE STATIONS OF DIFFERENT ELEVATIONS (SEE FIG. 1)

Station	Code	Elevation (m)	Windspeed (knots) +1 h	+2 h	+3 h	Mean
München-Riem	MR	530	18	17	12	16
Hohenpeißenberg	HP	977	27	24	21	24
Gr. Arber	AR	1437	38	33	(29)	33
Wendelstein	WS	1832	36	26	25	29
Zugspitz	ZU	2960	14	17	22	18

Only a little amount of mesoscale information is available from above. The satellite image taken by NOAA-9 at 1415 UTC exhibiting the bulge-shaped rim of a mesoscale complex of cloud with tops above 8 km has already been mentioned. A slight, but distinctly visible change in contrast can also be recognized in the infrared images obtained by METEOSAT, lying roughly along the tenth meridian at 12 UTC and somewhat further east and more curved at 15 UTC, remarkably close to the surface-front positions given in Fig. 3. As surface-front positions and lateral boundaries of distinct cloud complexes do not coincide in general, we conclude that the Papal Front in its developed state was strong enough to be manifest throughout a large portion of the troposphere. But, when looking at Europe as a whole, we recognize widely differing cloud structures. In the 15 UTC image a broad band of bright (i.e. high) cloud tops extended from Finland across Poland towards the Alps, apparently aligned with the synoptic-scale front discussed at the beginning of this section, whereas post-frontal cumulus complexes were present over France. The only remaining source of data consists in the regular European rawinsonde network. Making good use of that seems to be the only way to learn more about the processes that initiated the Papal Front.

4. Synoptic-scale environment aloft

For the assessment of the atmospheric flow field over Europe the application of an optimum interpolation scheme, which takes into account all available aerological data, appears to be superior to the somewhat arbitrary cross-sections through just a few rawinsondes, as presented by Heimann and Volkert (1988, Figs. 2, 3). Thus, we apply an objective analysis scheme to the mass and the wind fields on isentropic surfaces (Bleck 1975), and then use these data as input for a numerical integration using an adiabatic (dry) and hydrostatically balanced model in order to infer the synoptic-scale ageostrophic circulation, especially its vertical component. Specifically, a comparative numerical simulation is carried out to isolate orographic effects by replacing the model Alps by a plateau of the same elevation as the north Alpine foreland (550 m, see Fig. 1). The numerical model has been developed by Bleck (1984) and applied to case-studies of cyclogenesis in the lee of the Alps by Tafferner (1988 and 1990).

The primary data-base stems from about 70 rawinsonde stations distributed over Europe and North Africa at the nominal times 00 and 12 UTC 3 May, and 00 UTC 4 May. From this, the Montgomery potential and winds are analysed on isentropic surfaces (spaced at 2.5 K) with a horizontal resolution of about 50 km on a stereographic grid. As an additional diagnostic tool, potential vorticity on isentropic surfaces is used, defined by

$$P = -g(\zeta + f) \Big/ \frac{\partial p}{\partial \theta}, \tag{1}$$

where g, ζ, f, $\partial p/\partial\theta$ denote the earth's gravity, the relative vorticity on an isentropic surface, the Coriolis parameter, and the local change of pressure through potential temperature θ (a term closely related to static stability), respectively. Following the suggestion of Hoskins *et al.* (1985), potential vorticity is expressed in units of $10^{-6}\,\mathrm{m^2\,s^{-1}\,K\,kg^{-1}}$ (= 1 PVU). The forecast model integrates the primitive equations on 20 isentropic levels (the specific non-equidistant values are the isentropic levels as analysed in Figs. 11 and 13) and operates on the analysis grid. We carry out a simulation over 36 hours starting from 00 UTC 3 May, and determine vertical velocity fields from the vertical displacement of isentropic surfaces with time, as the vertical velocity itself is not a prognostic variable of the hydrostatic model. The orography for both analysis scheme

and prediction model is taken as an envelope from heights with 5′ resolution in latitude and longitude. Alpine model peaks attain 2500 m.

The 305 K isentropic surface, which is situated well within the middle troposphere at this time of year and in the geographic area under consideration (see also Fig. 11), is chosen to represent the synoptic situation over Europe. In Fig. 9, the evolution (time increment: 12 h) of the wind and potential vorticity fields are displayed. The outstanding feature is an isolated potential vorticity maximum (PVM), which is connected to a cyclonic synoptic-scale shortwave disturbance. During the first 12 h, from 00 UTC to 12 UTC on 3 May the PVM moved towards the south-south-east and its eastern edge lay just above the western rim of the Alps. During the following 12 hours, the PVM proceeded further towards the south-south-east over the western Alps and reached the northern part of the Mediterranean area. The horizontal winds were forced to circle around the PVM (see the discussions centring around the invertibility principle and associated scale effects in Hoskins *et al.* 1985), which acted as an upper-level cyclone. As pointed out by Tafferner (1988) such a PVM is not to be understood as a 'solid block', but rather is made up of individual parcels, each one characterized by the value of its potential vorticity. As the parcels move under the influence of the external forces the PVM as a whole undergoes rotation and translation, whereby at a later time the PVM is made up of the same parcels as before but with their positions changed relative to each other. The situation presented in Fig. 9 is an example of an outbreak of potential vorticity from its 'reservoir' within the polar stratosphere, as discussed by Hoskins *et al.* (1985). The maximum value of more than 6 units is exceptionally large for the 305 K isentropic surface.

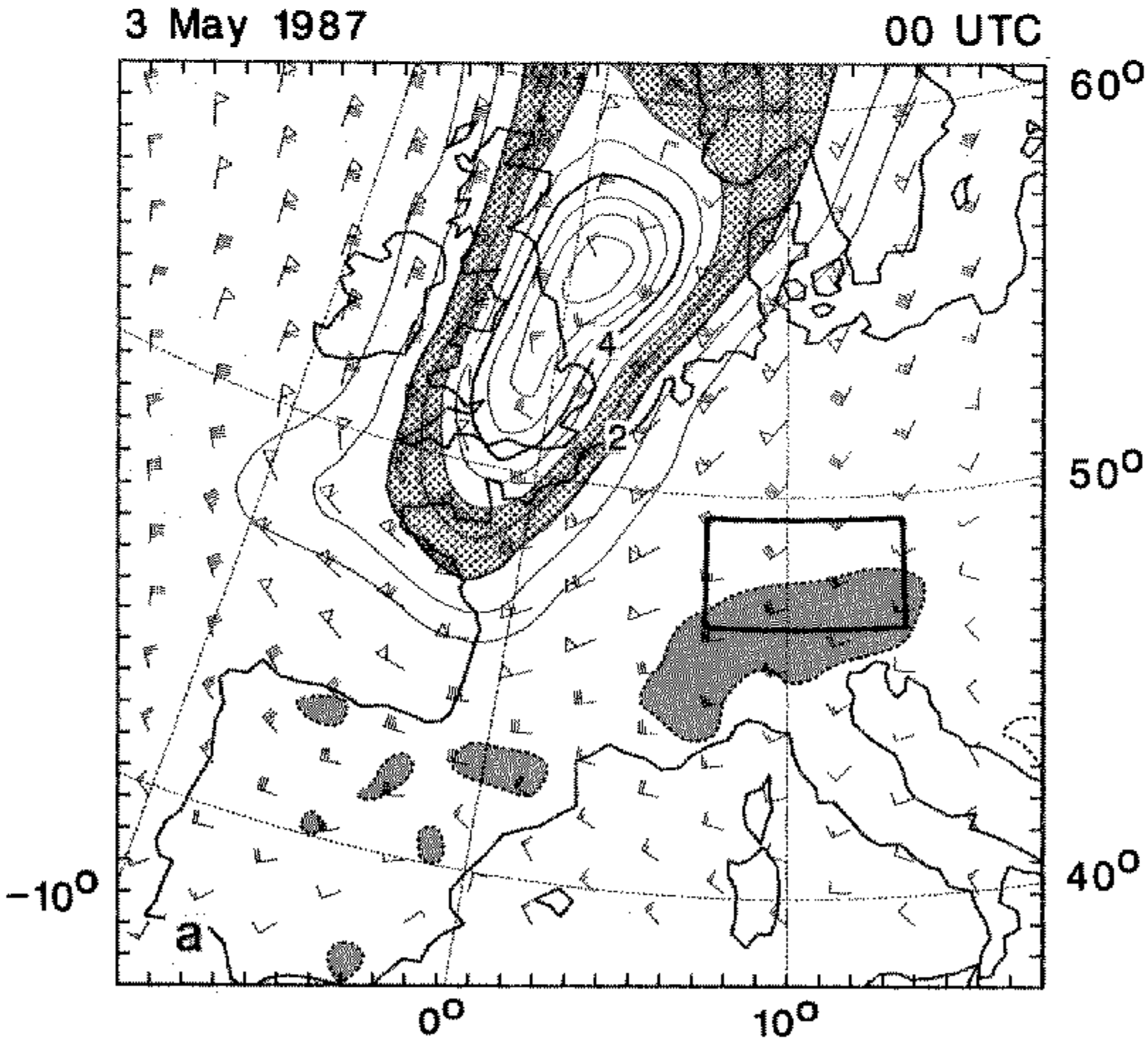

Figure 9. Objective analysis of potential vorticity (unit: $10^{-6}\,m^2\,s^{-1}\,K\,kg^{-1}$; isoline increment: 0.5 unit; the transition zone between low tropospheric and high stratospheric values is dotted) and horizontal wind (standard notation; in knots) on the mid-tropospheric isentropic surface $\theta = 305$ K for: (a) 3 May 1987, 00 UTC and (b) 12 UTC; (c) 4 May 1987, 00 UTC. Regions where analysis scheme heights exceed 1500 m are shaded; the box indicates the domain of the mesoscale analyses (see Figs. 1–3).

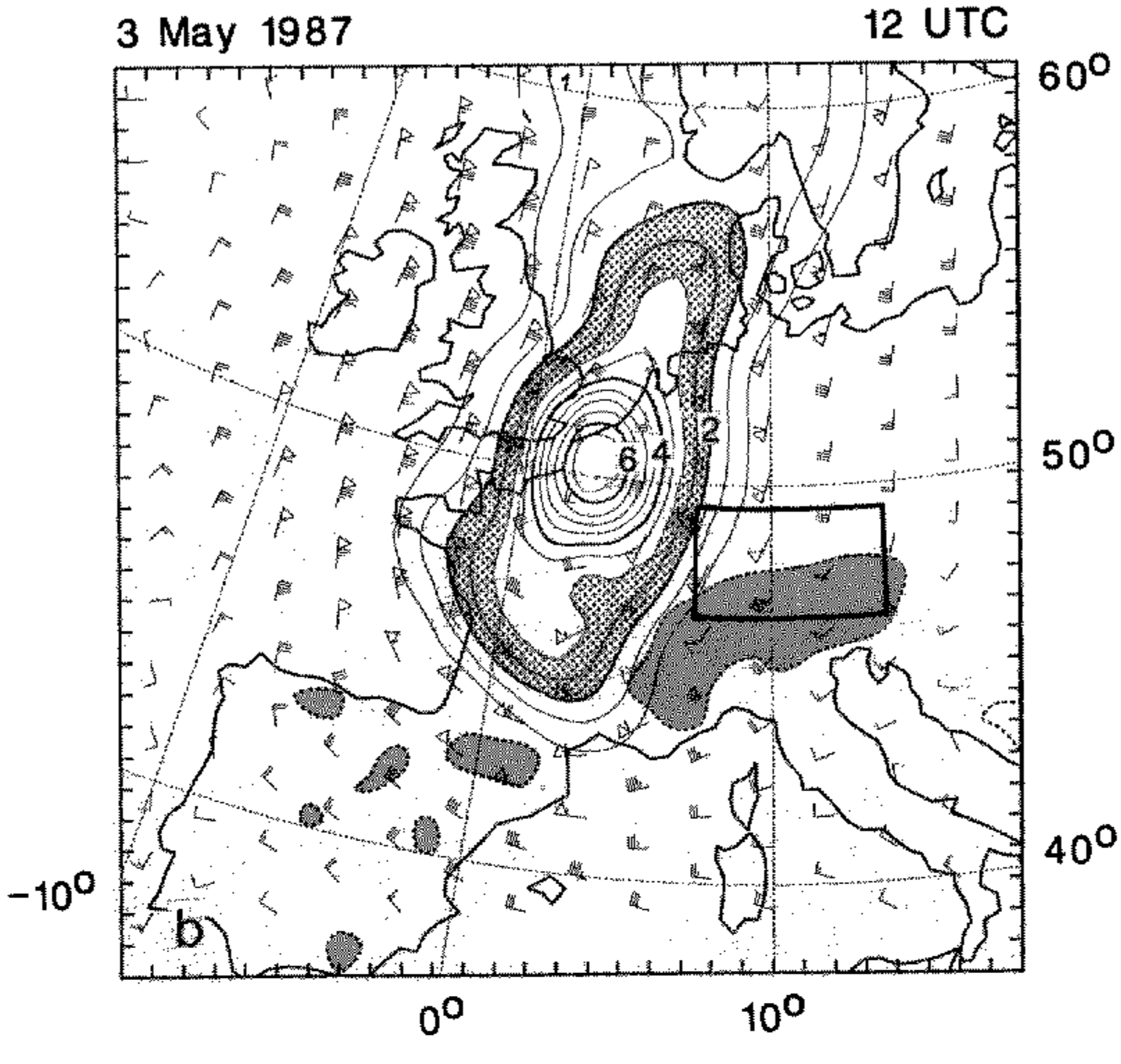

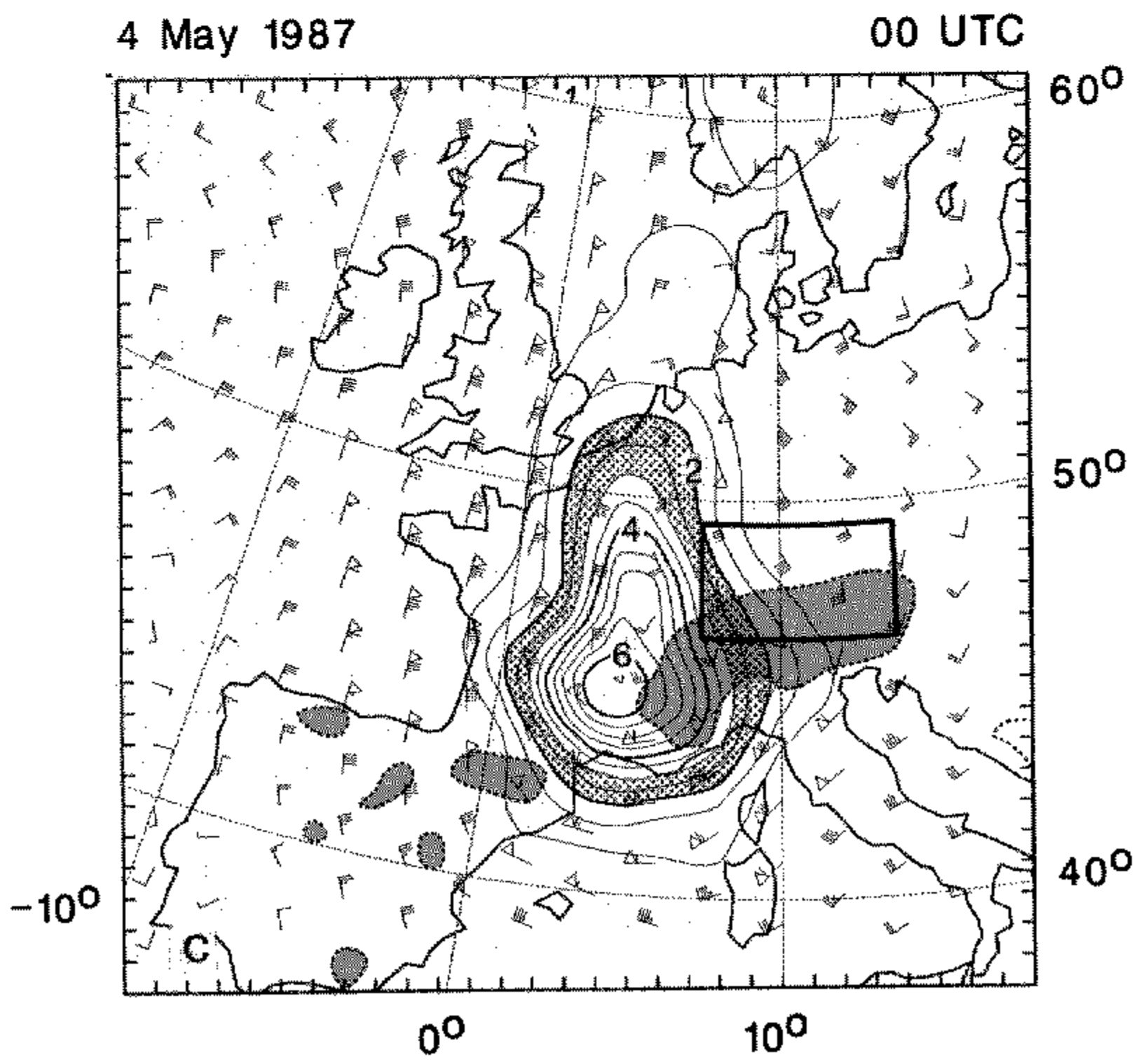

Figure 9. Continued.

The travelling PVM in the upper troposphere acts a 'guide' for a pool of cold air underneath it in the lower troposphere (see the discussion about outbreaks of cold air and potential vorticity against the Alps in Tafferner 1990). As the PVM approached the western edge of the Alps at about 12 UTC (Fig. 9(b)) the underlying cold air experienced blocking by the Alps, which led to the mesoscale high as displayed in Figs. 2(b) and 2(c). The orographic nature of this blocking at lower levels becomes more evident through a direct comparison of model results from simulations with full and 'cut-off' Alpine orography, respectively. The easterly advancement of the synoptically forced temperature contrast over central Europe caused by the Alpine barrier is shown in Fig. 10(a) for the 850 hPa level (approx. 1500 m a.m.s.l.; compare equally labelled dashed and full lines). The furthest advancement (approx. 200 km) is observed close to the model orography, but throughout the region of special interest (dashed box) the respective full lines lie further to the east. Furthermore, there is a cell of cold air ($\theta < 282$ K) at the north-western flank of the model Alps. It must be stressed that the dry and hydrostatic model with a grid size of about 50 km is not able to produce frontal gradients as concentrated as those observed at the surface (see Fig. 2) and most probably also existing at the 850 hPa level.

In addition to the eastward shift of the isentropes along the Alps, i.e. to an increase of zonal wind, we find the field of vertical velocity distinctly disturbed by the mountains (Fig. 10(b)). For the simulation with 'cut-off' Alps an elongated band of upward motion ($w > 4\,\mathrm{cm\,s^{-1}}$, shaded area) extends along the warm side of the temperature gradient. The Alpine block, when introduced fully, creates three cells alternating in ascent and descent in that region, which now lies in the lee of the mountains. Additionally, a broad band of orographic uplift is observed along the northern rim, with highest value in the cold region at the north-western flank. So, the low-level conditions are modified on both sides of the Alps. On the lee side, a centre of upward motion gets shifted over the Po

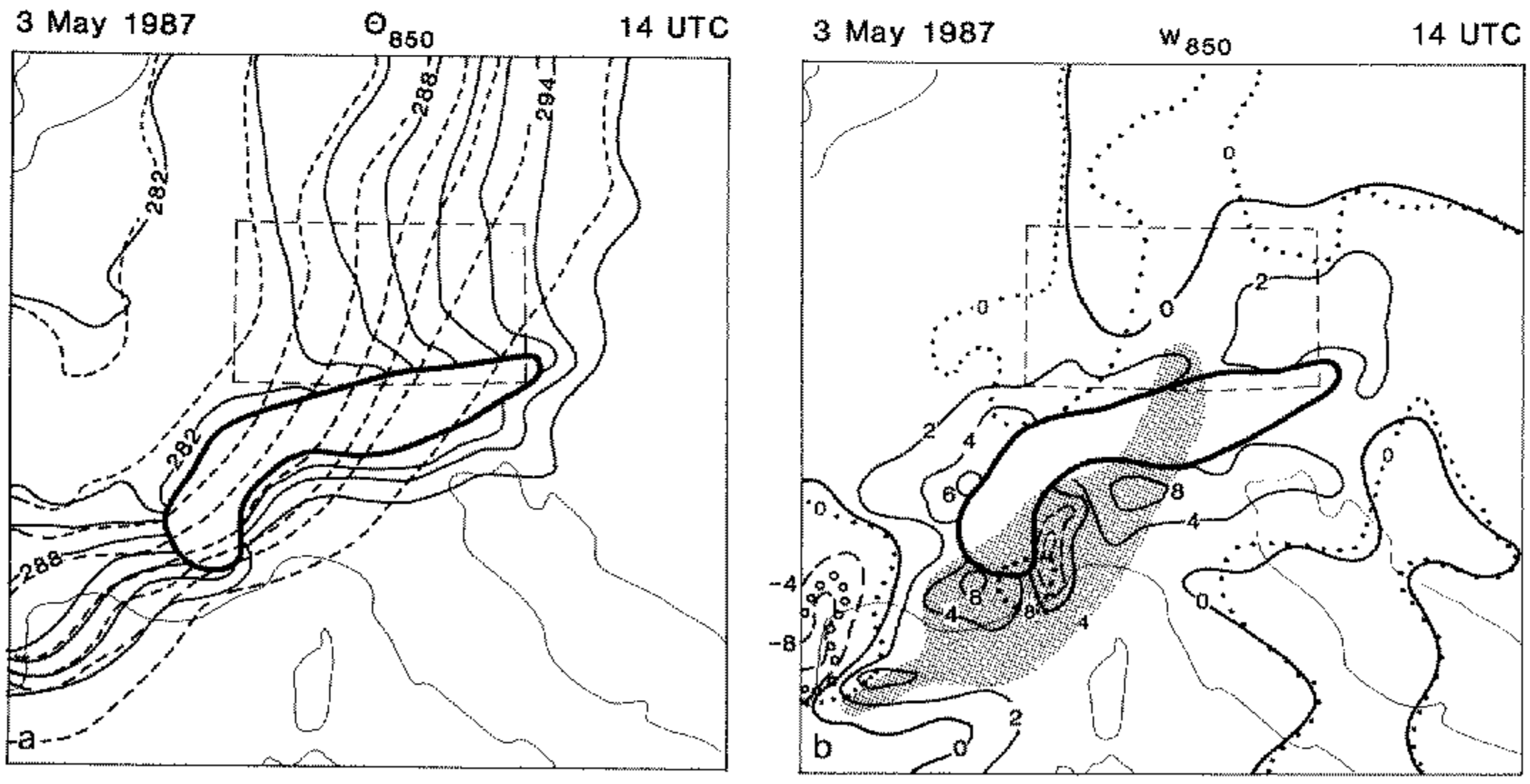

Figure 10. Lower tropospheric variables on the 850 hPa pressure surface as forecast by the model for 3 May 1987, 14 UTC for: (a) isentropes (increment: 2 K) for calculation with complete (full lines) and with cut-off Alpine orography (550 m; dashed lines); and (b) vertical velocity (increment: $4\,\mathrm{cm\,s^{-1}}$; $2\,\mathrm{cm\,s^{-1}}$ north of the Alps) for calculation with complete (full/dashed lines for positive/negative values) and with cut-off Alpine orography (550 m; dots/circles for positive/negative values; the region with $w > 4\,\mathrm{cm\,s^{-1}}$ is shaded). The heavy line indicates the intersection of the 850 hPa level and the Alps, inside which no values are defined for the calculation with mountains.

valley; it appears to be related to the lee cyclone which was about to evolve in the model and in reality, at the same location and with similar intensity. In the windward region orographic uplift is produced which may serve as a trigger for deep convection.

At 14 UTC, the orographic lifting produced by the model for the 850 hPa level is less pronounced in the area of special interest (where the Papal Front was about to pass Munich) than further to the south-west. A west–east cross-section at this time along the Alpine baseline (see Fig. 11) provides some more insight. Displayed are the non-equidistantly spaced isentropes (which are used as coordinate surfaces in the numerical model), potential vorticity and the ageostrophic circulation within the section. Note the dome of cold air in the western half, the 'roof' of which coincides at the 500 hPa level with the significantly lowered tropopause, which is marked by a thin layer of potential vorticity values between 2 and 3 PVU. Within that dome we find westward-directed, quasi-horizontal ageostrophic motion as is regularly the case in cyclonically curved flows where the observed winds are parallel to, but weaker than, the geostrophic winds. In the eastern part of the section the isentropes come down to the elevated terrain, resulting in a horizontal temperature gradient of about 10 K per 150 km. The salient feature, however, appears to be the tube of upward motion from about 750 hPa right into the

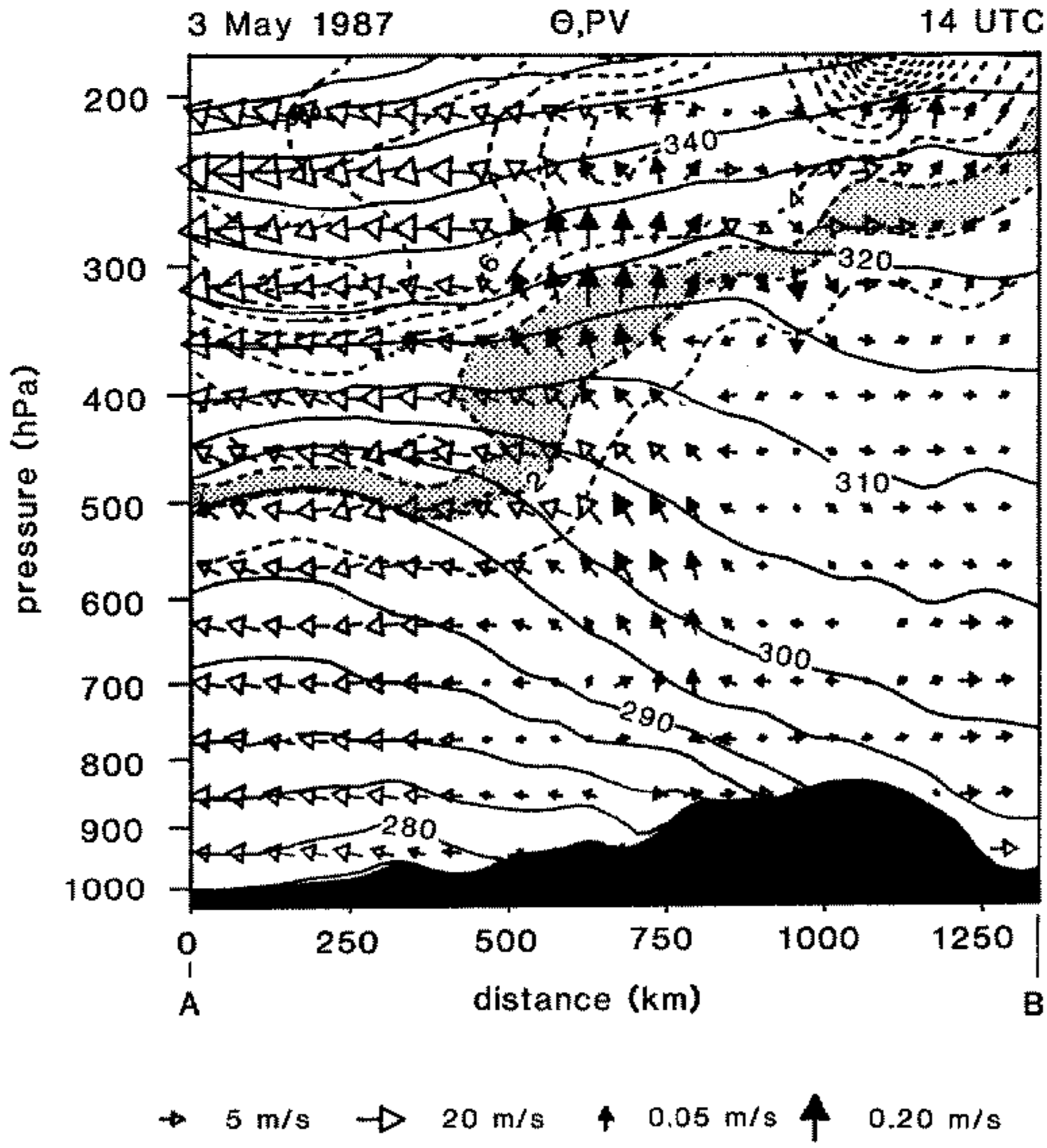

Figure 11. West to east cross-section along the northern flank of the Alps (see Fig. 12(b), A–B) for 3 May 1987, 14 UTC. Displayed are isentropes (solid lines with variable contour interval: $\Delta\theta = 2.5, 5, 10$ K), potential vorticity (dashed lines; units as in Fig. 9; increment: 1 unit; transition zone between tropospheric and stratospheric values shaded), model orography (black) and ageostrophic winds within the section (area of arrows proportional to speed, vertical component multiplied by 100; white/black arrows indicate predominant horizontal/vertical ageostrophic motion).

lower stratosphere above 300 hPa. The vertical velocity exceeds 10 cm s^{-1}. We explain this feature as a combination of two effects. In the middle troposphere (below, say 400 hPa) the upward motion is closely linked to the propagating PVM (see Fig. 9); in other words, we see synoptic-scale lifting ahead of a moving trough. The upper part of the tube of ascent is assumed to be associated with a jet streak embedded in the jet region, which was curved around the upper-level trough. What evidence is there to back such as assumption?

For judging the midday conditions at upper levels we use a manual analysis of geopotential and windspeed at the 300 hPa level (Fig. 12(a)) and model output of Montgomery potential and windspeed on the neighbouring 315 K isentropic surface (Fig. 12(b)). For the respective height coordinates both potentials are exactly equivalent for deducing the geostrophic wind (see e.g. Pichler 1986, p. 213 and p. 239). The former is constructed taking into account temporal consistency with the previous and subsequent charts (06, 18 UTC) and spatially interpolating windspeed between soundings by gradient wind evaluations. An extraordinarily narrow trough*, which developed into a cut-off low later on, lay with its centre over the Belgian coast having a band of high windspeed ($v > 80$ knots) around it, in which streaks of still faster flow ($v > 100$ knots) were embedded. The streak just off the north-western flank of the Alps is of special importance for our investigation. Fig. 12(b) illustrates to what extent the model reproduces these upper-level characteristics 12 hours after it was initialized. The gross features (position of trough centre, maximum windspeed) are well captured, but significant differences are evident. In the model, the trough is clearly wider, its gradient is somewhat weaker (4000 $m^2 s^{-2}$ compared to 4700 $m^2 s^{-2}$; note that the isoline increments in Figs. 12(a) and 12(b) are different) and the jet band does not extend right round the trough. Yet, a streaky maximum lies over the western Alps and moves over the area of special interest during the following model hours in a way similar to how the manually analysed streak had travelled on till 18 UTC (chart not displayed). At 14 UTC the exit region of the modelled streak was above the Alpine foreland where it produced a cell of considerable divergence, coinciding nicely with the upward motion at that time and place (see Fig. 11).

Collecting the aforementioned features together, we conclude that even in a simulation without moist processes several synchronous effects provided an exceptional synoptic-scale forcing for deep convection over the Alpine foreland: e.g. orographic blocking and lifting at low levels, ascent ahead of a potential vorticity maximum in the middle troposphere and the exit region of a jet streak at upper levels. All three components may be common features of the airflow near the Alps, but their simultaneous occurrence in the same region is likely to be a rare event. Of course, moist and mesoscale processes aloft, which could not be simulated in the present study, certainly played a major role in the energetic evolution which the Papal Front underwent after it was initiated by synoptic-scale forcing.

Finally, we check whether the model simulation gives any indication of an orographic jet over the forelands and below crest height. In Fig. 13, meridional cross-sections (see Fig. 12(b) for positions C and D) with isentropes and isotachs as of 17 UTC are juxtaposed for the simultations with full and 'cut-off' orography. Where the conditions in the upper troposphere are very similar, an extended region of positive zonal velocity below 800 hPa exists only in the simulation with full Alps (shaded region with $u > 7.5$ m s^{-1}). Just over the model Alps (700 hPa level above the 500 km tick mark) zonal speed is considerably lower in the simulation with full orography (4 m s^{-1} as opposed to 15 m s^{-1}). So, a low-

* Compare e.g. with the so-called *Vorderseiten*-type lee cyclogeneses during the ALPEX special observing period as documented by Lanzinger *et al.* (1990).

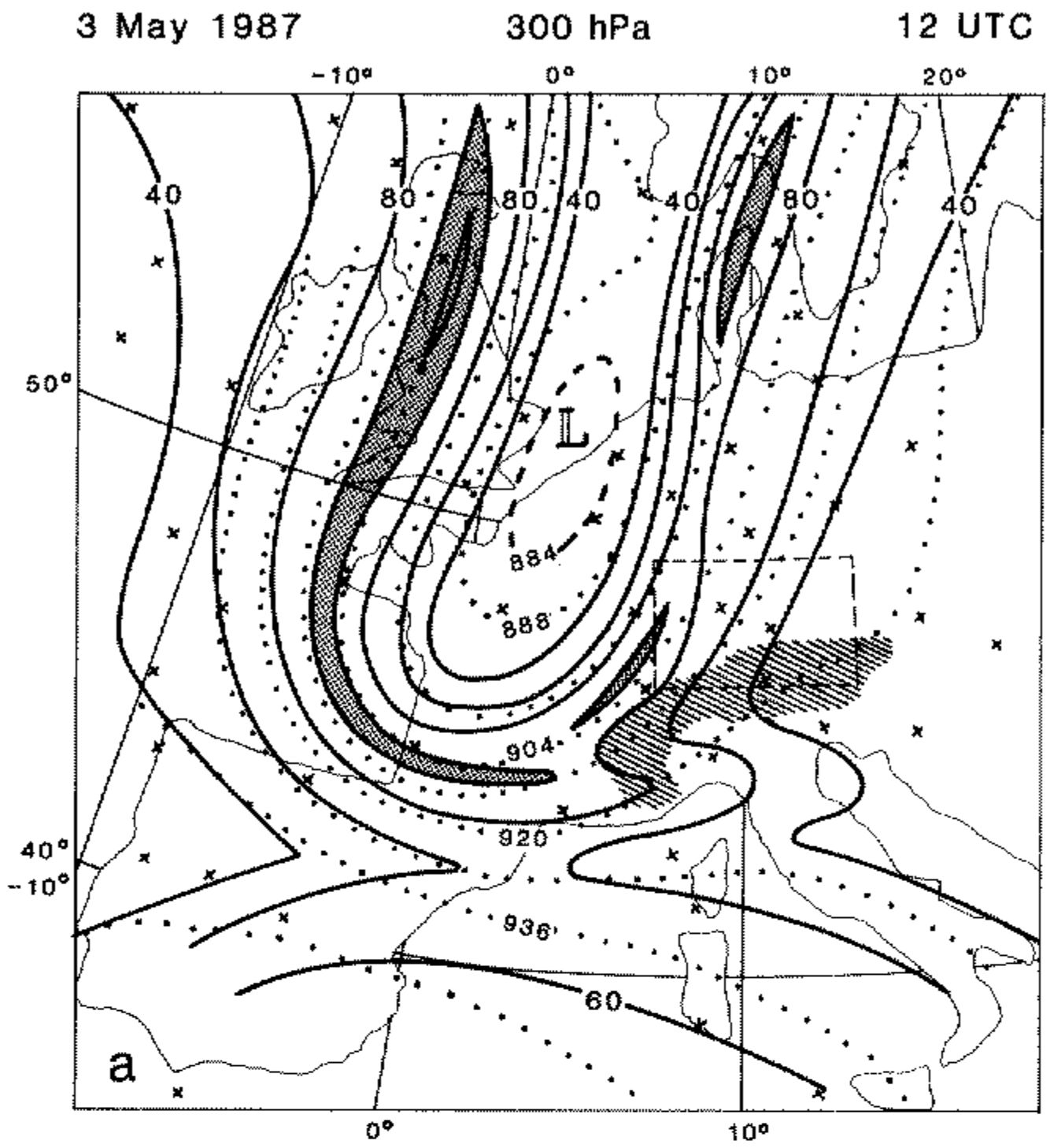

Figure 12. Upper tropospheric mass field and jet streaks for 3 May 1987, 12 UTC: (a) manual analysis of isotachs (knots; full lines) and geopotential (gpdam; dots) on the 300 hPa pressure surface; crosses denote rawinsonde stations; and (b) 12-hour model forecast of isotachs (knots; full lines and Montgomery potential ($10^3\,m^2\,s^{-2}$; dots) on the 315 K isentropic surface. Letters A, . . . , D denote end-points of the cross-sections in Figs. 11 and 13. Areas with $v > 100$ knots (jet streaks) are shaded, the Alpine arc is hatched and the box indicates the domain of the mesoscale analyses (see Figs. 1–3).

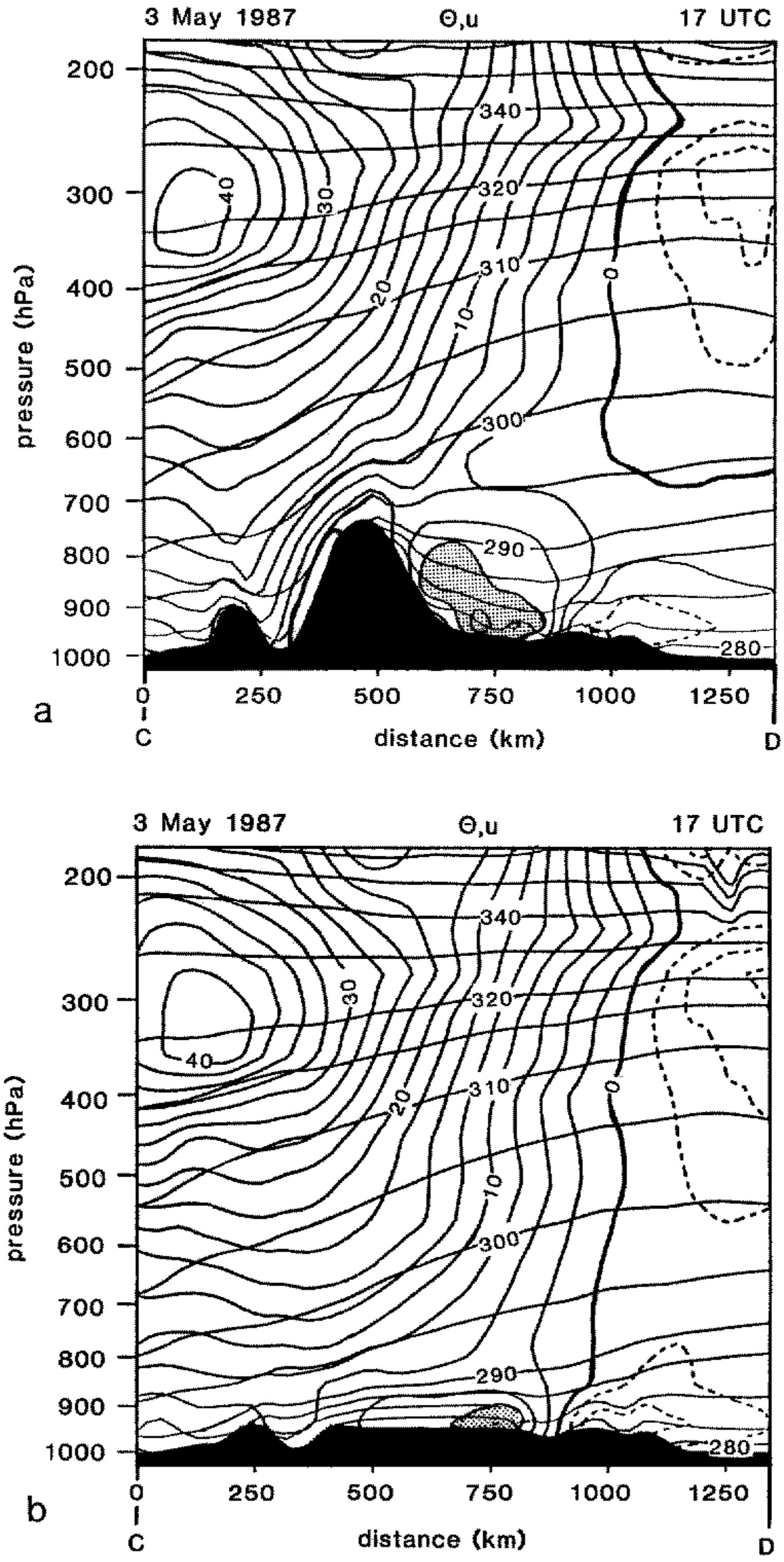

Figure 13. South to north cross-section along 10°E (see Fig. 12(b); C–D) as forecast by the model for 3 May 1987, 17 UTC. Displayed are isentropes (quasi-horizontal lines with variable contour interval: $\Delta\theta = 2.5$, 5, 10 K) and meridional wind component (quasi-vertical lines; increment: 2.5 m s^{-1}; negative values dashed; the region with $u > 7.5$ m s^{-1} near the ground is shaded) for calculation with complete (a) and with cut-off orography (b).

level jet is present in the simulation, but only if the Alpine orography is taken into account. Its vertical and meridional extent fits very well with the observations given in Table 3, but its calculated strength amounts only to about 50% of the observed values. In summary, we regard the observational and numerical evidence as sufficient for the classification of the orographic jet behind the Papal Front as a real feature.

5. Concluding remarks

In the previous sections we used two approaches to investigate the Papal Front of 3 May 1987, viz. mesoscale analyses of surface data and synoptic-scale objective analyses based on the regular European rawinsonde network in combination with adiabatic model simulations. Such a procedure is pragmatic as it uses the data and tools which are accessible and inevitably incomplete, e.g. the certainly important moist processes were not taken into account in the simulations. In the following we summarize our findings and look for links with other studies that emphasize the importance of diabatic processes for frontogenesis.

The mesoscale analyses of surface data revealed that during the morning hours of 3 May 1987 the Papal Front developed over south-western Germany as a secondary cold front and progressed eastward along the Alpine baseline while intensifying and accelerating. South of the river Danube and from 12 UTC onwards, a distinct wind squall was observed at the leading edge. The formation of deep convection and the release of conditional instability is indicated by reports of thunderstorms, short-period precipitation in excess of $50\,\mathrm{mm\,h^{-1}}$ and a cloud mass with elevated tops and a sharp and curved leading edge with the same position as the surface front. North of the river Danube, widespread and more persistent rain was observed with precipitation rates below $10\,\mathrm{mm\,h^{-1}}$.

The scarcity of mesoscale data from above for that particular day necessitated the use of the European radiosonde network, although this does not allow mesoscale features to be resolved. As a kind of data assimilation scheme, integrations of an adiabatic and hydrostatic numerical model were undertaken to obtain consistent fields of quantities which are not directly measured (e.g. the ageostrophic circulation), and for times between the synoptic hours. A comparative run with the Alpine orography 'cut-off' shed some light on the influence that the Alps exerted on the development. It is concluded that synoptic-scale forcing *and* orographic effects were both crucial (but certainly not sufficient) for the development of the Papal Front. The former comprises the advancement of a potential vorticity maximum and a pronounced shortwave trough towards the north-western flank of the Alps in a way that is termed *Vorderseiten*-type in studies classifying Alpine lee cyclogeneses (Pichler and Steinacker 1987). A propagating jet streak in the upper levels is considered to be a second important source of ascent above the Alpine foreland. The orographic influence acted particularly at lower levels through blocking effects and the evolution of an orographic jet below crest height. Although this study concentrated on the evolution of pronounced mesoscale features north of the Alps, it should be kept in mind that the synoptic-scale forcing also led to the formation of a lee cyclone over the Mediterranean later on. Furthermore, the crucial importance of the region along the north-western rim of the Alps for subsequent developments is documented once more (compare e.g. Pichler and Steinacker 1987, Fig. 8 for a case of pronounced flow-splitting in the lower troposphere and Kurz 1990, Fig. 4 for diagnosed frontogenesis at lower levels in this region).

At this point, it becomes apparent that a considerable gap exists between our mesoscale analyses which document the overall effects of the Papal Front, and some

synoptic-scale driving mechanisms as revealed by the simulation. Thermodynamic processes certainly were important for the fierce development as a squall-type front close to the Alps. Yet, we are not in a position to quantify them. Some time after the front had passed, precipitation turned into snow even at the ground. Szeto *et al.* (1988) showed by two-dimensional simulations that the extraction of latent heat from the environmental air by the melting of snow can have a considerable frontogenetical effect. Also, similarities exist with a case-study of a mesoscale front with squall-line characteristics over the United States, for which radar data were throughly evaluated (Smull and Houze 1987) and two-dimensional simulations, including ice-phase processes, undertaken (Fovell and Ogura 1988). Detailed comparisons, however, are hardly possible as the available data and the geographic situations are too heterogeneous.

Somewhat more relevant to our case are two modelling studies, which were carried out recently by Heimann (1988 and 1990). The first considered the synoptic situation of the Papal Front using a three-layer model with a one-way nesting facility for the horizontal directions and a parametrization for liquid-water processes. It was shown that the Alpine orography led to an orographic jet and that even the crude representation of moist processes resulted in an enhanced frontal speed along the mountains. The second study investigated the propagation of synthetic cold fronts approaching the Alps from different directions by applying a fully three-dimensional hydrostatic gridpoint model with parametrizations for water-phase concentrations (including cloud-ice and snowflakes). Front type A, which had some similarities to the Papal Front (surface front from the west, prefrontal upper-level flow across the Alps from 210 degrees), proved to be strengthened by orographic effects (prefrontal warming due to Föhn conditions) *and* by post-frontal cooling through the evaporation of rain and the melting of snow within the sub-cloud layer. Thus, we can conclude that, on one hand, moist processes most certainly have contributed to the vigour which the Papal Front attained in its developed state but that, on the other hand, special synoptic-scale and orographically induced processes were necessary to initiate the development. Future case-study-type numerical experiments with this more advanced model could be used to quantify the above distinction.

More generally, this case-study demonstrates the amount of detailed surface observations which are available for the Alpine region from routine sources, however diverse. Combined with the regular aerological information, a data-base is in principle at hand which could be exploited for a whole series of case-studies in order to infer the relative importance of particular frontal events. The spatial and temporal resolution of the Alpine data can easily compete with those obtained along other mountain ranges. Nevertheless, special experimental efforts are necessary, if the gap between mesoscale information from the surface and less-well-resolved data from higher levels is to be bridged. Finally, we anticipate that a well-balanced combination of data evaluations taken from both routine sources and special campaigns, and careful numerical experimentation will eventually widen our knowledge in the complex field of atmospheric fronts influenced by orography.

Acknowledgements

Case-studies crucially depend on accessible observational data. Therefore, we want to express our gratitude to all colleagues who supplied us with data, specifically the staff of the Central Office of the Deutscher Wetterdienst in Offenbach, its Regional Offices in Freiburg, Munich, Nuremberg, and Stuttgart, the Observatory on the Hohenpeißenberg, and of the observing station in Constance. Valuable information was also provided by F. Fiedler (Karlsruhe), H. Lößlein (Garching), and H. Scheffold (Oberpfaf-

fenhofen) as well as by Austrian colleagues from observing stations in Innsbruck, Linz Salzburg, and St. Pölten. V. Zwatz-Meise (Vienna) kindly provided Meteosat images. A. Waldvogel (Zürich) quickly made available the Swiss radar images after we had heard about them at the very end of this study. The cooperation is acknowledged of J. Colquhoun and R. Steinacker who contributed the information for Table 1 which was not available from their publications. J. Freund, A. Hart and G. Jacob gave valuable assistance during the preparation of the figures. Detailed comments from M. Reeder and anonymous reviewers helped significantly to clarify the line of argument.

References

Austin, P. M. 1987 Relation between measured radar reflectivity and surface rainfall. *Mon. Weather Rev.*, **115,** 1053–1070

Bleck, R. 1975 An economical approach to the use of wind data in the optimum interpolation of geo- and Montgomery potential fields. *Mon. Weather Rev.*, **103,** 807–816

1984 An isentropic coordinate model suitable for lee cyclogenesis simulation. *Riv. Meteorol. Aeronaut.*, **43,** 189–194

Bosart, L. F., Pagnotti, V. and Lettau, B. 1973 Climatological aspects of eastern United States backdoor cold frontal passages. *Mon. Weather Rev.*, **101,** 627–635

Carr, J. A. 1951 The east coast "backdoor" front of May 16–20, 1951. *Mon. Weather Rev.*, **79,** 100–105

Clough, S. A. 1987 The mesoscale frontal dynamics project. *Meteorol. Mag.*, **116,** 32–42

Colquhoun, J. R., Shepherd, D. J. Coulman, C. E., Smith, R. K. and McInnes, K. 1985 The Southerly Buster of southern Australia: an orographically forced cold front. *Mon. Weather Rev.*, **113,** 2090–2107

Egger, J. 1987 Distortion of fronts near orography. *Meteorol. Rdsch.*, **40,** 141–146

1989 Föhn and quasi-stationary fronts. *Beitr. Phys. Atmos.*, **62,** 20–29

Fovell, R. G. and Ogura, Y. 1988 Mesoscale circulations forced by melting snow. Part II: application to meteorological features. *J. Atmos. Sci.*, **45,** 3846–3879

GARP 1986 'Scientific results of the Alpine experiment (ALPEX)'. GARP Publ. Ser. No. 27, WMO, Geneva.

Griffiths, R. W. and Hopfinger, E. J. 1983 Gravity currents moving along a lateral boundary in a rotating fluid. *J. Fluid Mech.*, **134,** 357–399

Hartjenstein, G. and Egger, J. 1990 Frontogenesis near steep orography. *Tellus*, **42A,** 259–269

Heimann, D. 1988 The "Papal Front" of 3 May 1987: modelling of orographic and diabatic effects. *Beitr. Phys. Atmos.*, **61,** 330–343

1990 Three-dimensional modeling of synthetic cold fronts approaching the Alps. *Meteorol. Atmos. Phys.*, **42,** 197–219

Heimann, D. and Volkert H. 1988 The "Papal front" of 3 May 1987—mesoscale analyses of routine data. *Beitr. Phys. Atmos.*, **61,** 62–68

Hoinka, K. P. 1985 On fronts in central Europe. *Beitr. Phys. Atmos.*, **58,** 560–571

Hoinka, K. P. and Heimann, D. 1988 Orographic channelling of a cold front at the Pyrenees. *Mon. Weather Rev.*, **116,** 1817–1823

Hoinka, K. P. and Volkert H. 1987 The German front experiment 1987. *Bull. Am. Meteorol. Soc.*, **68,** 1424–1428

Hoinka, K. P., Hagen, M., Volkert H. and Heimann, D. 1990 On the influence of the Alps on a cold front. *Tellus*, **42A,** 140–164 (Palmén special issue)

Höller, H. and Reinhardt, M. E. 1986 The Munich hailstorm of 12 July 1984—convective development and preliminary hailstone analysis. *Beitr. Phys. Atmos.*, **59,** 1–12

Hoskins, B. J., McIntyre M. E. and Robertson, A. W. 1985 On the use and significance of isentropic potential vorticity maps. *Q. J. R. Meteorol. Soc.*, **111,** 877–946

James, P. K. and Browning, K. A. 1979 Mesoscale structure of line convection at surface cold fronts. *Q. J. R. Meteorol. Soc.*, **105,** 371–382

Joss, J. and Waldvogel, A. 1990 Precipitation measurement and hydrology. Pp 577–606 in *Radar in meteorology.* Ed. D. Atlas. American Meteorological Society, Boston.

Kurz, M. 1990 The influence of the Alps on structure and behaviour of cold fronts over southern Germany. *Meteorol. Atmos. Phys.*, **43,** 61–68

Lanzinger, A., Pichler, H. and Steinacker, R. 1990 ALPEX-Atlas, Innsbruck. (Obtainable from Institute of Meteorology and Geophysics, Univ. Innsbruck, Innrain 52, A-6020 Innsbruck)

Mahoney, W. P. III 1988 Gust front characteristics and the kinematics with interacting thunderstorm outflows. *Mon. Weather Rev.*, **116,** 1474–1491

Mass, C. F. and Albright, M. D. 1987 Coastal southerlies and alongshore surges of the west coast of North America: evidence of mesoscale topographically trapped response to synoptic forcing. *Mon. Weather Rev.*, **115,** 1707–1738

Parish, T. R. 1982 Barrier winds along the Sierra Nevada mountains. *J. Appl. Meteorol.*, **21,** 925–930

Pichler, H. 1986 *Dynamik der Atmosphäre.* 2nd ed., B.I. Wissenschaftsverlag, Bibliographisches Institut, Mannheim

Pichler, H. and Steinacker R. 1987 On the synoptics and dynamics of orographically induced cyclogenesis in the Mediterranean. *Meteorol. Atmos. Phys.*, **36,** 108–117

Ryan, B. F., Wilson, K. J., Garratt, J. R. and Smith, R. K. 1985 Cold fronts research programme: progress, future plans, and research directions. *Bull. Am. Meteorol. Soc.*, **66,** 1116–1122

Shapiro, M. A., Hampel, T., Rotzoll, D. and Mosher, F. 1985 The frontal hydraulic head: a micro-α scale triggering mechanism for mesoconvective weather systems. *Mon. Weather Rev.*, **113,** 1166–1183

Smull, B. F. and Houze, R. A. 1987 Rear inflow in squall lines with trailing stratiform precipitation. *Mon. Weather Rev.*, **115,** 2869–2889

Staude, R. 1970 Der Hagelsturm am 6. Juli 1968 im Kreis Landsberg am Lech. *Meteorol. Rdsch.*, **23,** 48–53

Steinacker, R. 1987 Orographie und Fronten. *Wetter und Leben*, **39,** 65–70

Steiner, J. T., Revell, C. G., Ridley, R. N., Smith, R. K., Page, M. A., McInnes, K. L. and Sturman, A. P. 1987 The New Zealand southerly change experiment. *Bull. Am. Meteorol. Soc.*, **68,** 1226–1229

Szeto, K. K., Stewart, R. E. and Lin, C. A. 1988 Mesoscale circulations forced by melting snow. Part II: application to meteorological features. *J. Atmos. Sci.*, **45,** 1642–1650

Tafferner, A. 1988 'Strahlstromstruktur und Leezyklogenese'. Ph.D. thesis, Universität München

1990 Lee-cyclogenesis resulting from the combined outbreak of cold air and potential vorticity against the Alps. *Meteorol. Atmos. Phys.*, **43,** 31–48

Volkert, H. 1989 The "Papal Front" of 3 May 1987—precipitation rates. *Meteorol. Rdsch.*, **41,** 121–125